# SYNTHESIS AND CHARACTERIZATION OF CROSSLINKED URETHANE DOPED POLYESTERS FOR VASCULAR TISSUE ENGINEERING

by

JAGANNATH DEY

Presented to the Faculty of the Graduate School of

The University of Texas at Arlington in Partial Fulfillment

of the Requirements

for the Degree of

MASTER OF SCIENCE IN BIOMEDICAL ENGINEERING

THE UNIVERSITY OF TEXAS AT ARLINGTON

December 2008

ACKNOWLEDGEMENTS

I would like to thank Dr. Jian Yang, for opening the door for me to work in his laboratory and being my advisor. His continuous support and belief in my abilities encouraged me to complete this thesis successfully. He always motivated me to reach my goal. He was also positive and optimistic about my results and lab work. I appreciate his suggestion, guidance, and patience throughout this work.

I would also like to thank Dr. Kytai Nguyen and Dr. Liping Tang for serving on my thesis committee and for permitting me to use their laboratory facilities during the course of my research. I would like to extend my thanks to Dr. Brent Sumerlin at Southern Methodist University for assisting us with the characterization. I would also like to appreciate all the help extended to me by Ashwin Nair and for being a continuous source of support and encouragement. I would like to express my sincere gratitude to Hao Xu, Dr. Jinhui Shen and Paul Thevenot for all their help in compiling this manuscript. I would like to sincerely thank my lab mates, in particular Vikas Kache, Richard Tran, Dipendra Gyawali and Yi Zhang for both their criticism and support in the lab. Lastly and most importantly, I thank my parents, Mr. Ratan Kumar Dey and Mrs. Anima Dey and my sister, Anamika Dey, for all their love and support in my efforts. Without their blessings, I would not have succeeded in my life.

November 25, 2008

ABSTRACT

SYNTHESIS AND CHARACTERIZATION OF CROSSLINKED URETHANE DOPED POLYESTERS FOR VASCULAR TISSUE ENGINEERING

Jagannath Dey, M.S.

The University of Texas at Arlington, 2008

Supervising Professor: Jian Yang

Traditional crosslinked polyester elastomers are inherently weak, and the strategy of increasing crosslink density to improve their mechanical properties makes them brittle materials. Biodegradable polyurethanes, although strong and elastic, do not fare well in dynamic environments due to the onset of permanent deformation. The design and development of a soft, strong and completely elastic (100% recovery from deformation) material for tissue engineering still remains a challenge. Herein, we report the synthesis and evaluation of a new class of biodegradable elastomers, crosslinked polyurethane-doped polyesters (CUPEs), which is able to satisfy the need for soft, strong, and elastic biomaterials. Tensile strength of CUPE was as high as 41.07±6.85 MPa with

corresponding break strains of 222.66±27.84%. The Young's Modulus ranged from 4.14±1.71 MPa to 38.35±4.5 MPa. Mechanical properties and degradation rates of CUPE could be controlled by varying the choice of diol used for synthesis, the polymerization conditions, as well as the concentration of urethane bonds in the polymer. The polymers demonstrated good *in vitro* and *in vivo* biocompatibility. Preliminary hemocompatibility evaluation indicated that CUPE adhered and activated lesser number of platelets compared to PLLA. Good mechanical properties and easy processability make these materials well suited for soft tissue engineering applications. The introduction of CUPEs provides new avenues to meet the versatile requirements of tissue engineering and other biomedical applications.

TABLE OF CONTENTS

LIST OF ILLUSTRATIONS

LIST OF TABLES

# CHAPTER 1

# INTRODUCTION

## 1.1 Importance of Vascular Tissue Engineering

It is estimated that nearly 1 in 3 adults in America alone suffer from one or more forms of cardiovascular disease (CVD) (AHA statistics). Atherosclerosis, both in forms of coronary artery and peripheral vascular disease, is one of the most severe forms of CVD and is responsible for 50% of all deaths in the United States, Japan and Europe [1]. The disease pathology includes the narrowing of arteries by the formation of atherosclerotic lesions and plaque formation in the blood vessels. This lesion continues to grow in size until it obstructs the flow of blood through the blood vessel. If the vessel in question is a coronary artery, the subsequent blockage of the vessel leads to a weakened myocardium and finally to a myocardial infarction [2]. In order to restore the blood supply, bypass surgeries are performed. The current treatment modalities for bypass surgeries include a. Use of autologous veins and arterial grafts [3]; b. Use of synthetic prosthetics like expanded polytetrafluoroethylene and Dacron. Table 1.1 summarizes these different treatment schemes.

It may be noted from Table 1.1 that synthetic prosthetics are less than satisfactory when used as small diameter vascular replacements. In order to engineer more suitable small diameter blood vessels, it is necessary that we first understand its design requirements.

Table 1.1 Comparison between Autologous venous/arterial grafts with synthetic prosthetics

| **Autlogous veins and arteries** | **Pros** |
|---|---|
| Surgical bypass of the obstructed vessel with autologous vein or arterial grafts remains the standard treatment procedure for artherosclerosis [3]. In particular, the saphenous veins and internal mammary arteries [4] are the representative substitute for small diameter vascular reconstruction. The most important problem associated with these constructs is their availability, surgical cost of graft harvesting and donor site morbidity [5]. The use of alternate treatments like use of synthetic prosthetics is considered only when autologous vessels are either damaged or unavailable. | √ Bypass using autologous veins and arteries does not necessitate use of anti-rejection therapies.<br>√ Ideal mechanical properties which are similar to those of the vessel being replaced. These grafts are suturable.<br>√ 3-D structure and the presence of all the cellular and protein components allows for excellent integration at the implant site and immediate graft functionality.<br>√ Autologous veins and arteries can be used immediately after harvesting.<br>√ These grafts can be remodelled in vivo and hence are suitable for implantation in pediatric patients as well. |
| | **Cons** |
| | x Unavailable in cases of previous harvesting, trauma or due to damage to these vessels as a result of disease pathology.<br>x Harvesting of these vessels leads to donor site morbidity. [5]<br>x High surgical costs are associated with harvesting the desired autologous vessel [6]. |
| **Synthetic Prosthetics (ePTFE, Dacron)** | **Pros** |
| Synthetic prosthetics are resorted to only upon the unavailability of autologous blood vessels. This is because of their poor properties in comparison with vein | √ Easily available and scalable technology<br>√ Has shown long term patency in |

| | |
|---|---|
| Table 1.1 - continued<br><br>and arterial grafts. Small diameter blood vessels prepared using these prosthetics fail due to thrombotic complications. Different strategies like a. Seeding endothelial cell monolayer [7]; b. Coating lumen with biodegradable polymers [8]; and c. Binding anti-coagulants like heparin, hirudin to graft lumen [9] have been used to improve patency in below knee configurations by reducing thrombogenicity. Modified prosthetics have higher patency owing to the reduced thrombogenic complications. | medium (6-10 mm) and large diameter (>10mm) blood vessel replacement.<br>√ Good suturability and suture retention<br><br>**Cons**<br><br>x Unsuitable for pediatric patients, since these grafts have no growth potential.<br>x Poor patency demonstrated when used as small diameter vascular grafts (<6mm) [10]. This has primarily been attributed to thrombosis.<br>x Prosthetic material properties do not match that of native vessels. Neither ePTFE or Dacron exhibit viscoelasticity. The utilization of these grafts also leads to anastomotic intimal hyperplasia due to mismatch in material properties. |

## 1.2 Requirements of an Ideal Vascular Graft

For successful revascularization, a synthetic prosthetic graft should be able to mimic the functionality and the properties of native vasculature. After intensive reviews of successes and failures, a list of criteria which must be fulfilled by a prosthetic to successfully act as a small diameter blood vessel substitute has been drawn up [4, 11-15]. These include

a. ***Biocompatibility (including Hemocompatibility):*** The prosthetic must be compatible with cells, tissues and blood in order to function properly and avoid thrmobotic complications. Vascular cells must be able to populate the conduit and

produce similar quantities of collagen and elastin as is seen in native vessels. Complete endothelium formation should be possible in the graft lumen.

b. ***Similarity in Design and Construction:*** The prosthetic must be similar to an autologous vessel in terms of its construction and make up. Large blood vessels in the body have three distinct layers, namely, tunica intima, tunica media and tunica adventitia. Each of these layers is comprised of different cell types, which are isolated from each other by an elastic lamina. Tunica intima forms the luminal surface with endothelial cells, tunica media comprises of circumferentially arranged smooth muscle cells and the tunica adventitia comprises of fibroblasts. For a synthetic prosthetic to achieve long term patency, its construction should allow for the growth, differentiation and isolation of these different cell types.

c. ***Mechanical Properties:*** Blood vessels are soft yet, tough and elastic contructs. The ultimate elongation of arteries and veins has been reported to approach 260% under tensile forces [16]. The material used to fabricate the prosthesis should be soft, have high tensile strength and elasticity. Moreover, the material should also be resistant to cyclic deformations since the blood vessels are under a constant cycle of compression and relaxation [17]. The deviation in the properties of the prosthetic material from native vasculature results in compliance mismatch which further leads to myointimal hyperplasia especially at the site of the anastomosis, which is a major reason for graft failure. Additionally, the graft material should also be tough to ensure that it may be sutured into place [18, 19].

d. ***Ease of Processing:*** The prosthetic must be easily processable into different dimensions and architectures depending on the site of implantation. For example, small blood capillaries lack the well defined design of the larger arteries described above. Ease of processing is essential to be able to meet all the overall requirements of the vessel being replaced.

Currently, no prosthetic grafts are able to meet these requirements and there is a void in the availability of a suitable synthetic substitute for a small diameter blood vessel. Owing to its success in the repair of burns [6, 20] , chronic wounds [21] and on an experimental level, cartilage defects [22], it is widely believed that tissue engineering may hold the key to developing a vascular graft which fulfills all these requirements.

## 1.3 Tissue Engineered Blood Vessels (TEBVs)

In recent times the principles of tissue engineering have been applied to the problem of developing a small diameter vascular graft. The tissue engineering approach relies upon the seeding of a tubular construct and either allowing the cells to mature in vitro prior to implantation or implanting the seeded construct to allow in vivo remodeling of the seeded cells. The premise for using tissue engineering is that the grafts produced by this method would be living grafts [23], capable of responding to the immediate transplant environment. These grafts could therefore be remodeled by the host and conduct self repair upon damage. The task of engineering a blood vessel is severely complicated by the complex design and construction of native vasculature. Moreover, for

certain tissue engineering applications the graft is allowed to be remodeled in vivo prior to expression of functionality. TEBVs however, have to be functional immediately after transplantation leading to further complications in the fabrication of a TEBV.

As observed earlier with endothelialized prosthetics, although the presence of a functionalized endothelium may alleviate thrombotic complications, an implant may fail if its properties do not resemble that of native vessels due to compliance mismatch and onset of anastomotic intimal hyperplasia. Therefore, the choice of an appropriate scaffold material is crucial to the success of a tissue engineered graft upon implantation. As of date, four different types of materials have been used by tissue engineers for designing an appropriate scaffold with varying degrees of success. These scaffold candidates include a. Natural proteins b. Decellularized matrices c. Cell sheets and d. Biodegradable/non-biodegradable polymeric scaffolds.

### *1.3.1 Natural Protein Scaffolds*

The premise for using natural proteins like collagen and elastin is their abundance and structural importance in native blood vessels. The combined effect of stiff collagen fibers and elastic elastin proteins are responsible for the unique viscoelastic properties of vasculature [24]. Since Weinberg and Bell demonstrated a tubular scaffold exhibiting arterial architecture made of Collagen I gel [25], different researchers have attempted to use collagen gels as templates for tissue engineered blood vessels [26-29]. The pros and cons of using these native proteins as matrix templates have been summarized in Table 1.2.

Table 1.2 Pros and Cons of using natural proteins as matrices for tissue engineered blood vessels.

| Pros | Cons |
|---|---|
| 1. Cells seeded collagen gels mimic the in vivo environment, wherein cells are surrounded by matrix proteins.<br>2. Cells are able to bind to the proteins via membrane receptors. This allows cells to migrate and remodel the scaffold. [30, 31]<br>3. Collagen can be obtained in large quantities by biopsies and foreskin isolation among other methods [33]. | 1. Demonstrate poor intraluminal burst pressure strengths [25, 26].<br>2. Collagen gels limit mechanical properties by attenuating collagen synthesis by fibroblasts and smooth muscle cells [32]. Poor mechanical strength necessitates the use of a synthetic support, like Dacron as sleeves.<br>3. Mechanical strength may be improved by crosslinking collagen. However, commonly used crosslinkers like carbodiimides and aldehydes are toxic [34, 35]. |

Various techniques have been attempted in order to improve the mechanical properties of these collagen seeded gels. These include a. using reducing sugars for crosslinking collagen [36]; b. Mechanically stimulating seeded cells to orient circumferentially and secrete both collagen and elastin [28, 29]; c. Using collagen/elastin blends instead of pure collagen gels as templates [37] d. Electrospinning collagen/elastin to produce nanofibrous matrices [38, 39]. Other natural proteins like fibrin [32, 40] and fibrin/collagen blends [41] have also been used for vascular tissue engineering.

### *1.3.2 Decellularized Matrices*

Decellularized extracellular matrices (ECMs) of porcine and canine origin have also been used as blood vessel templates [42-45]. The rationale behind using decellularized

matrices is that the decellularization procedure removes all xenogenic cellular components leaving behind a non antigenic ECM for cellular repopulation [46, 47]. No antigens are expressed by the ECM proteins and hence it cannot trigger an immunogenic response. The advantages and disadvantages of using these xenogenic matrices are highlighted in Table 1.3.

Various strategies have been utilized by different research groups in order to overcome the deficiencies of these decellularized grafts. These include a. Use of water soluble carbodiimides instead of gluteraldehyde as crosslinking agents to remove residual cytotoxicity [44]; b. Seeding of autologous endothelial cells on the lumen of the decellularized matrices prior to implantation, rather than allowing for in vivo endothelialization [43, 45]; c. Development of more standardized and automated processing techniques to reduce the variability in the ECM obtained from different donors [24].

In spite of these modifications, this technique of using decellularized tissues as blood vessels has not been able to demonstrate patency greater than 130 days [45].

Table 1.3 Pros and Cons of using decellular vascular tissues as scaffolds for tissue engineered vascular grafts.

| **Pros** | **Cons** |
|---|---|
| 1. Decellularized ECMs preserve the three dimensional architecture of native blood vessels [48]. | 1. The decellularization procedure may weaken the extracellular matrix and necessitate further steps to strengthen it [44] |

| | |
|---|---|
| Table 1.3 - continued | |
| 2. The ECM contains structural proteins like collagen and elastin which the cells can recognize and bind with. Moreover, the proper alignment of these proteins ensures that the matrices have mechanical properties similar to that of native vasculature. The presence of these fibrillar proteins also ensures that these scaffolds demonstrate good initial strength and suturability [44, 47]. | 2. Chemical crosslinking is the easiest mechanism to improve the mechanical properties of decellularized scaffolds. However, this may leave behind traces of toxic crosslinkers like gluteraldehyde, which harm cell attachment and growth [49]. |
| 3. This approach cuts down the time required to engineer arteries and is suitable for immediate implantation. | 3. The properties of the ECM obtained cannot be controlled. |
| 4. Xenogenic matrices are available in abundance. | 4. ECM obtained from different sources would be different from each other. Batch by batch variations would limit the scalability of this method.<br>5. This technique relies on vascular re-modeling in vivo, wherein the graft re-populates itself from circulating vascular cells. This process of in vivo vascular cell migration is not well understood [13] |

*1.3.3 Biodegradable Synthetic Polymeric Scaffolds*

The use of synthetic polymeric scaffolds in vascular tissue engineering has widely been explored in the search for a suitable material for fabricating small diameter vessel substitutes. In this direction, different research groups have used a variety of synthetic materials like polylactic acid (PLA) [50], polyglycolic acid (PGA) [51-53], polyhydroxyalkanoates (PHA) and polydioxanones (PDS), either by themselves or in conjugation with another polymer. However, the performance of these materials has been far from satisfactory. Polyglycolic acid and polylactic acid degrade between 2 weeks to 2

months respectively depending on the molecular weight of the polymer [54]. This short duration is insufficient for graft maturation and leads to failure of vessels fabricated using these materials. Additionally, the degradation products of these polymers cause the microenvironment to become acidic and instigate an inflammatory response [39]. In order to overcome these deficiencies, PLA and PGA have been used in the form of co-polymers or blends with other polymers, like PHAs [55] and polyurethanes [56]. Although the use of PDS demonstrated interesting results and patency up to one year in a rabbit aorta model [57], the mechanical properties of PDS differ from that of blood vessels. PDS is more often used in bone tissue engineering [58, 59] and this mismatch in properties is expected to affect long term patency due to compliance issues.

Biochemical and mechanical interactions between cells and the underlying extracellular matrix (ECM) are two primary factors governing healthy cell growth, differentiation and functionality [60-62]. For cells seeded on a synthetic scaffold used for tissue engineering, the scaffold must provide cues similar to those exchanged between native tissue and ECM. One strategy aimed at fulfilling this requirement, involves the use of scaffolds, which are analogous to the ECM of the target tissue in terms of its mechanical, physical, and chemical properties. To better mimic the ECM and transfer mechanical stimulation from the tissue surroundings to the seeded cells, the scaffold has to be soft and elastic. Additionally, scaffolds for engineering soft tissues should be elastic, so that they are able to sustain and recover from cyclic deformations which are characteristic of these mechanically active tissues.

It was realized that the existing materials were hard and brittle and hence more suitable for engineering tissues like bone, which require high strength and modulus. The field of "soft tissue engineering" was introduced in order to develop soft, elastic and yet strong materials which would be more compliant with tissues like nerves, cardiac tissue, bladder and blood vessels. Due to their elasticity, such polymers were referred to as elastomers. Biodegradable elastomers broadly include two families, a. crosslinked network polyesters like poly(glycerol sebacate) (PGS) [63] and poly(octane diol citrate) (POC) along with its corresponding family of polymers [64] and b. biodegradable poly(ester urethanes) [65-67].

## 1.4 Family of Poly(Diol Citrates)

Poly(diol citrate) is a family of thermoset network polyester elastomers developed by Yang et al [64]. The synthesis of POC is carried out by the condensation polymerization of equimolar ratios of a diacid, namely citric acid and a diol. The representative reaction schematic is indicated in Fig 1.1 with 1,8-octane diol as the diol monomer. At the end of the reaction, a thermoplastic pre-polymer is obtained which, has to be crosslinked by oven curing into order to obtain the thermoset polymer. In the pre-polymer form the poly diol citrates may be molded into a variety of different shapes and geometries. Poly diol citrates have good mechanical properties, with tensile strength ranging from 2.93±0.09MPa to 11.15±2.62 MPa. The mechanical properties may be controlled by the choice of diol used in the synthesis and the temperature and duration of oven crosslinking. Owing to the presence of crosslinking, poly diol citrates are 100% elastic

and regain their original dimensions after the release of stress factors acting upon them. This family of materials also demonstrates excellent cell/tissue compatibility which has been demonstrated in both, *in vitro* and *in vivo* studies [64, 68]. Hemocompatibility evaluation of POC indicated that POC adhered and activated lesser number of platelets compared to both, PLGA and ePTFE which are FDA approved blood contacting materials [69]. Additionally, human aortic endothelial cells and human aortic smooth muscle cells were also found to proliferate on POC [68].

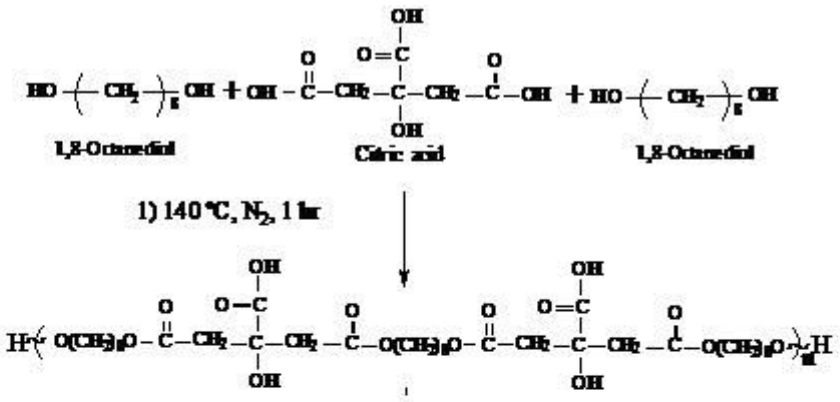


Fig 1.1 Reaction schematic for synthesis of poly(1,8-octane diol) citrate

evaluation of POC indicated that POC adhered and activated lesser number of platelets compared to both, PLGA and ePTFE which are FDA approved blood contacting materials [69]. Additionally, human aortic endothelial cells and human aortic smooth muscle cells were also found to proliferate on POC [68].

After demonstrating the suitability of POC as a good blood contacting biomaterial, further work was concentrated on the development of a biphasic tubular

scaffold to function as a synthetic vascular graft [17]. The scaffold had a non porous inner lumen and a porous outer layer to isolate the HAECs from the HASMCs. The scaffolds had higher burst pressure compared to systolic pressure for arteries in the body. In addition, the biphasic grafts demonstrated compliance of 12.7% which was similar to that of canine and human carotid artery. This further indicated that POC coupled with the biphasic scaffold design may be a potential solution to the in vitro fabrication of synthetic vascular grafts.

As a suitable material for vascular tissue engineering, POC fulfills the requirements of biocompatibility, hemocompatibility, and compliance. However, it fails to function as a successful graft in vivo owing to its poor mechanical properties and poor suturability. Although POC films have excellent tensile properties, the porous POC scaffolds are weaker and retain only 8.5% of the strength of the POC films. It is possible to increase the strength of the polymer by increasing the duration of post polymerization. However this approach would also result in over-crosslinking the material and compromising its elasticity. Therefore, in order to take advantage of POC as a vascular replacement material, other methods have to be explored in order to increase the strength of POC.

## 1.5 Biodegradable Polyurethanes

Polyurethanes are a family of block co-polymers which have been used for biomedical applications for over three decades [70]. Polyurethanes are synthesized from three components, namely a polyol, a diisocyanate and a chain extender. A typical synthesis reactions comprises of a polyol-diisocyanate reaction in the first step to form

the pre-polymer which is subsequently chain extended to form the high molecular weight polyurethane. Polyurethanes exhibit a segmented architecture, wherein the diisocyanate and chain extender form the hard segments of the polymer chain and the interspersed polyol sections form the soft segments. The block architecture comprising of alternating blocks of hard and soft segments is responsible for the wide range of elastomeric properties exhibited by this material. The soft segments, owing to their low glass transition temperatures are responsible for the elasticity of the polymer. The hard segments on the other hand, make the polymer stiffer due to the presence of inter-chain hydrogen bonds between the hard segment urethane bonds of the different polymer chains. The hydrogen bonding causes the hard segments to pack themselves into crystalline domains which function as physical crosslinks between the polymer chains, thus imparting stiffness to the polymer. In addition to producing a material which is both elastic and strong, this architecture is able to produce a wide range of mechanical properties by a. varying the ratio of the hard segment to the diol b. varying the choice of the hard segment and soft segment components.

Owing to their good biocompatibility and inherent elastomeric properties, it was expected that polyurethanes would be more suitable than ePTFE and Dacron in resolving issues of compliance [18] and therefore increasing patency. Different commercial forms of polyurethane grafts like the Corvita graft [71] the Cardiotech graft [72] have shown very promising results with patency upto 3 years in a canine model, and are currently under clinical trials. The non biodegradable and permanent nature of these implants however, restricts the use of these implants to old age patients. Moreover, in order to

make these polyurethanes resistant to degradation, potentially toxic diisocyanates like toluene diisocyanate are used for the synthesis. Studies have also indicated that slow degradation results in the release of carcinogenic compounds like toluene diamine in animal models [54].

Biodegradable polyurethanes have thus gained popularity over the past decade. These polymers use non toxic diisocyanates like lysine diisocyanate (LDI) and hexamethylene diisocyanate (HDI), and degrade into harmless compounds [73-75]. These biodegradable polyurethanes can serve as temporary elastomeric scaffolds for the tissue engineering of living vascular grafts which are capable of remodeling and growth. Guan et al. have synthesized and characterized polyester(urethane-ureas) (PEUUs) for the purpose of vascular tissue engineering [65, 66]. Scaffolds fabricated using PEUUs have tensile strengths of up to 1 MPa and elasticity of 213% [76]. In a recent study, a tubular PEUU scaffold was seeded with muscle derived stem cells and kept in culture for a period of 7 days. The cell seeded construct suppored cell growth, attachment and proliferation and had a burst pressure of 2127±900 mmHg and suture retention strength of 1.3±0.3 N, which are close approximates of native blood arteries [77].

In spite of the recent successes of biodegradable polyurethanes in the fabrication of a tissue engineered vascular graft, some important issues still remain unaddressed. One of the most important drawbacks of polyurethanes includes mechanical deformation under cyclic stresses due to the aliphatic structure [78]. Blood vessels are mechanically active tissues which are under constant cyclic loading. The use of polyurethanes for such applications without resolving the issue of permanent creep would result in reduced

patency in an in vivo environment. Another important issue which needs to be addressed is the slow degradation rates of polyurethanes. The urethane linkages of polyurethanes are resistant to hydrolytic scission and hence these polymers degrade very slowly. faster degradation rates may be obtained by increasing the soft segment-hard segment ratio, but this would also make the polyurethane weaker. Hence, it is desirable to develop some means by which the degradation rate of the polymer may be controlled without affecting its mechanical properties significantly.

## 1.6 Objectives of this Research

### *1.6.1 Specific Aims*

Both crosslinked polyester networks, particularly poly(1,8-octane diol citrate) and biodegradable polyurethanes suffer from certain limitations in their application to vascular tissue engineering. POC has the advantages of excellent biocompatibility and hemocompatibility, controllable degradability and 100% recovery from deformation, while lacking good mechanical properties. Biodegradable polyurethanes on the other hand have excellent mechanical properties and good biocompatibility, but suffer from the onset of permanent creep and slow degradation. The goal of this research is to design and develop a new polymer which is able to combine the properties of both, POC and biodegradable polyurethanes. The specific aims pursued in this study included

a. Aim 1: Synthesize and characterize a new polymer which combined the properties of crosslinked polyester networks and polyurethanes.

b. Aim 2: Evaluate the biocompatibility and hemocompatibility of this new polymer, ensuring its suitability for vascular tissue engineering.

The successful **outcome** of this research project would provide a new biodegradable polymer, which would be able to satisfy the needs of controllable biodegradability, strong and elastic tensile properties, good biocompatibility and hemocompatibility. It is also expected that this material can be fabricated into tubular scaffolds for vascular tissue engineering.

# CHAPTER 2

# SYNTHESIS AND CHARACTERIZATION OF CUPE POLYMERS

## 2.1 Introduction

Although POC is a strong, totally elastic elastomer, it fails to retain its strength upon processing into porous scaffold structures. The peak stress of POC films was as high as 2.93±0.09 MPa. Upon fabrication into scaffolds however, the peak stress value dropped to 0.3±0.1 MPa. In order to make stronger scaffolds for more load bearing applications, it is therefore necessary to design elastomers with high degree of stiffness. This would ensure that the subsequent leftover mechanical properties upon processing the material into a scaffold would still meet the requirements of the desired application. The introduction of urethane linkages in the POC chain is one possible way to increase the mechanical properties. The urethane bonds are polar in nature and form strong inter-chain hydrogen bonds between the polymer chains, which are responsible for the improved mechanical properties. In order to introduce urethane linkages in POC, both ends of the POC chain must be capped with hydroxyl groups. This was achieved by the synthesis of POC using a slight excess of 1,8-octane diol. Hexamethylene diisocyanate (HDI) is the chain extender, which was chosen to extend the POC chain length. HDI was selected because of its frequent usage in the synthesis of various biodegradable polyurethanes [79-82]. HDI has also demonstrated in the formation of higher molecular weight polymers compared to other commonly used diisocyanates [79, 83].

In this set of studies, we synthesized and characterized a new polymer, crosslinked urethane doped polyesters (CUPEs), which comprises of long chains of POC bridged by urethane linkages. Different molar ratios of HDI to the diol component were used to examine the different degrees of chain extension on polymer properties. The aim of this portion of the study was to extensively investigate the properties of the different CUPEs and understand the effect of the isocyanate content in regulating material properties like mechanical properties, thermal properties and degradation rates of the different CUPE polymers.

## 2.2 Materials and Methods

### *2.2.1 Materials*

All chemicals, cell culture medium and supplements were purchased from Sigma-Aldrich (St. Louis, MO), except where mentioned otherwise. All chemicals were used as received.

### *2.2.2 CUPE Synthesis*

CUPE synthesis was carried out in three distinct steps (Fig 2.1). Step 1 involved synthesis of the POC pre-polymer. POC was synthesized as per previously published methods with slight modifications [84]. Briefly, citric acid and 1,8-octanediol, with a monomer ratio of 1:1.1 were bulk polymerized in a three necked reaction flask, fitted with an inlet and outlet adapter, at 160-165 °C. Once the mixture had melted, the temperature was lowered to 140 °C, and the reaction mixture was stirred for another 60

minutes to create the POC pre-polymer. The pre-polymer was purified by drop wise precipitation in deionized water. Undissolved pre-polymer was collected and lyophilized to obtain the purified POC pre-polymer. The average molecular weight of pre-POC was characterized as 1000 Da by Matrix assisted laser desorption/ionization mass spectroscopy (MALDI-MS) which was done using an Autoflex MALDI-TOF Mass Spectrometer (Bruker Daltonics, Manning Park, MA). Chain extension of the POC pre-polymer to obtain pre-CUPE was done in Step 2. Purified pre-POC was dissolved in 1, 4-dioxane to form a 3% (wt/wt) solution. The polymer solution was reacted with 1,6-hexamethyl diisocyanate (HDI) in a clean reaction flask under constant stirring, with stannous octoate as catalyst (0.1% wt). Different pre-CUPE polymers were synthesized with different feeding ratios of pre-POC:HDI (1:0.6, 1:0.9 and 1:1.2, molar ratio). The system was maintained at 55 °C throughout the course of the reaction.

Small amounts of the reaction mixture were removed at 6 hour intervals and subjected to Fourier transform infra red (FT-IR) analysis. The reaction was terminated when the isocyanate peak at 2267 cm-1disappeared. Step 3: The pre-CUPE solution was cast in a Teflon mold and allowed to dry in a chemical hood equipped with a laminar air flow until all the solvent had evaporated. The resulting pre-CUPE film was moved into an oven maintained at 80 °C for pre-determined time periods to obtain crosslinked urethane-doped polyester (CUPE).

The synthesis procedure was repeated with poly(ethylene glycol) (PEG) (Mw = 200) by replacing all or part of 1,8-octane diol as the diol portion. This class of CUPEs were abbreviated as CA-PEGUX/Y, where CA-PEGU refers to citric acid-PEG-urethane,

X/Y denotes the molar ratio of 1,8-octane diol to PEG used in the synthesis. For example, CA-PEGU8/3 indicates that 0.08 moles of 1,8-octanediol and 0.03 moles of PEG were reacted with 0.1 mole of citric acid. The molar ratio of the CA-PEGU pre-polymer:HDI was maintained at 1:0.9 for all the different variants.

## 2.3. Polymer Characterization

### *2.3.1 Infra-Red (IR) Measurements*

Fourier transform infra red (FT-IR) spectra were obtained using a Nicolet 6700 FT-IR spectrometer (Thermo Fisher Scientific) at room temperature. A dilute solution of CUPE and POC pre-polymers in 1,4-dioxane (3% wt/wt) was cast on KBr crystals and allowed to dry for 12 hours under vacuum before being used to obtain the spectra. Spectra were recorded after completion of 32 scans. Attenuated total reflectance spectroscopic analysis was performed using an IRAffinity-1 ATR spectrometer (Shimadzu Corp, Japan) on solvent cast CUPE and POC films which had been polymerized in an 80 °C oven for 2 days.

### *2.3.2 Thermal Analysis*

The thermal properties of the different CUPE polymers were evaluated using Differential Scanning Calorimetry (DSC) and Thermogravimetric Analysis (TGA). DSC was performed using a DSC2010 Differential Scanning Calorimeter, (TA Instruments, New Castle, DE) and Thermogravimetric Analysis (TGA) using a SDT2960

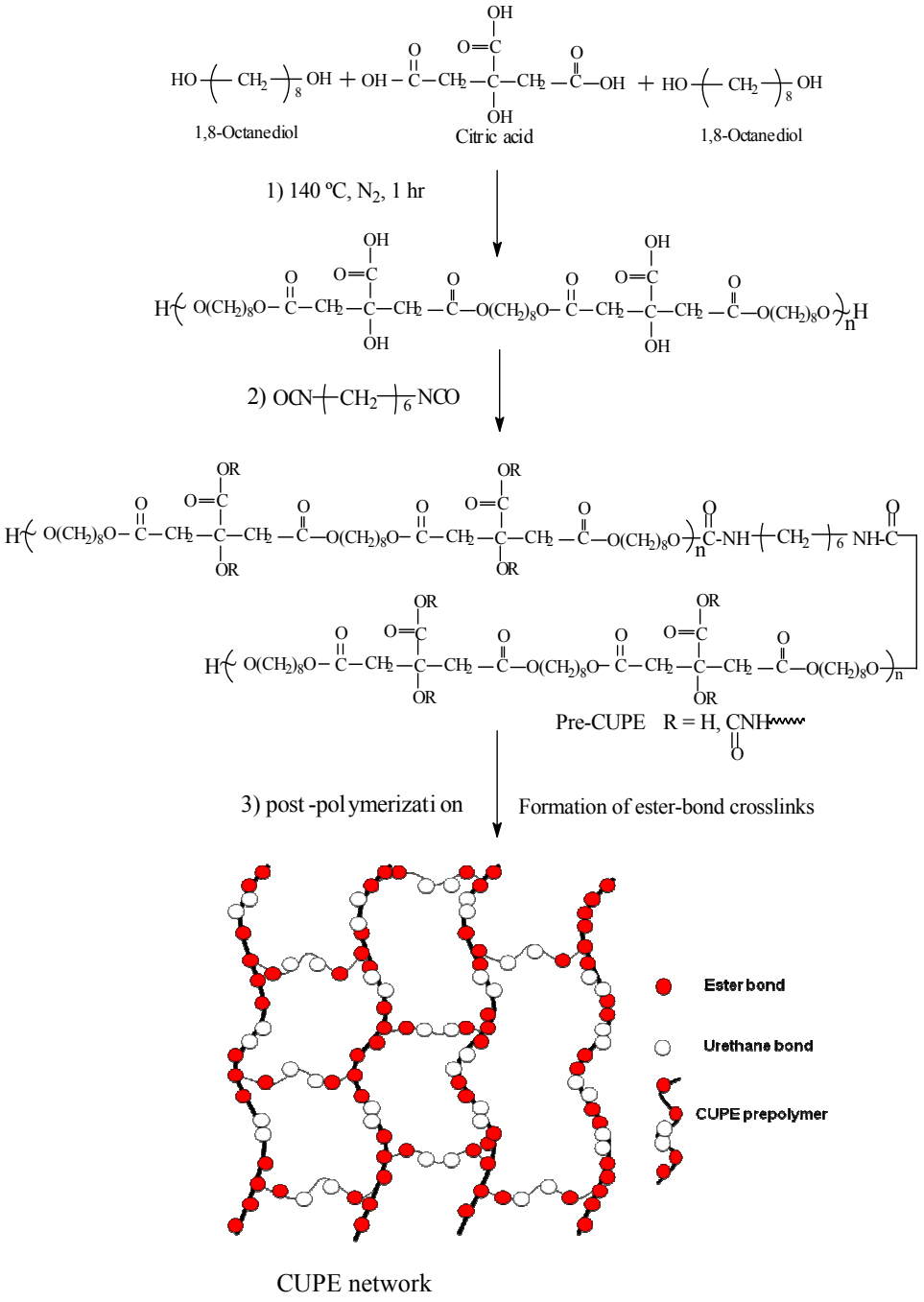


Fig 2.1 Synthesis schematic of CUPE polymers. The monomers citric acid and 1,8-octanediol underwent condensation polymerization to produce hydroxyl group capped poly(1,8-octanediol citrate) in step 1. In step 2, 1,6-hexamethyl diisocyanate was used to extend the POC chain; A schematic of the representative structure of CUPEs is also depicted.

Simultaneous DSC-TGA (TA Instruments, New Castle, DE). For DSC, the polymer samples were scanned to 150 °C under nitrogen with a step size of 10 °C/minute, followed by cooling at a rate of -40 °C/minute, until a temperature of -60 °C was achieved. Readings were then taken during a second heating scan from -60 °C to 230 °C, with a constant heating rate of 10 °C/minute. The glass transition temperature $T_g$ was determined from the middle of the recorded step change in heat capacity from the second heating run. For TGA, the polymer samples were heated at a rate of 10 °C/min from 50 °C to 600 °C, in an atmosphere of nitrogen gas. The temperature, at which 10% loss of the initial weight occurred, was recorded as the decomposition temperature $T_d$.

*2.3.3 Mechanical Properties*

Mechanical testing was conducted on an MTS Insight 2 machine fitted with a 500 N load cell. The samples were cut into a dog bone shape, as per ASTM D412a (25 x 6 x 1.5mm, length x width x thickness). The deflection rate was adjusted to 500 mm/min. Samples were elongated to failure. The Young's modulus was calculated by measuring the gradient in the initial linear region of the tensile curve. Five specimens per sample were tested and averaged.

*2.3.4 Density and Molecular Weight between Crosslinks ($M_c$)*

The density of the different polymers was measured by the fluid displacement method using a density measurement kit (Mettler Toledo, Columbus, OH). The auxiliary liquid used was de-ionized water.

Crosslink density and molecular weight between crosslinks was evaluated according to the theory of rubber elasticity [63, 64].

$$n = \frac{E_0}{3RT} = \frac{\rho}{M_c} \quad (1)$$

where n is the number of moles of active network chains per unit volume, $E_o$ is the Young's modulus of the polymer, R stands for the universal gas constant, T represents the absolute temperature, ρ is the density of the polymer and $M_c$ relative molar mass between crosslinks.

*2.3.5 Contact Angle Measurements*

Water in air contact angle measurements were made on CUPE thin films by sessile drop method, using a KSV101 Optical Contact Angle and Surface Tension Meter (KSV Instruments Inc. Helsinki, Finland). Readings were collected within 10 seconds after dropping. Eight readings were collected from different regions on the CUPE films.

*2.3.6 Wide Angle X-Ray Diffraction (XRD)*

X-ray scattering was used to detect the presence of crystallinity in the CUPE films using a wide angle X-ray diffraction apparatus (name of machine??). CUPE1.2 was used as the representative polymer for the examination. Thin films of CUPE1.2 were cast in a Teflon mold and allowed to post-polymerize for 4 days at 80 °C prior to the experiment. X-ray scans were collected over a 2θ range of 10° to 80° with a dwell time of 1s and increments of 0.2°.

*2.3.7 In Vitro Degradation*

Degradation studies were conducted in both phosphate buffered saline (PBS) (pH 7.4) and NaOH solutions (0.01 M and 0.05M). NaOH degradation was used to screen the polymer degradation in a relatively short period of time [64]. The polymer films were cut into 7 mm discs using a cork borer. The initial weights of the samples were noted, and they were placed in test tubes containing 10 ml of either PBS or NaOH and incubated at 37 °C for the period of the study. At pre-set time points, the samples were removed and washed thoroughly with de-ionized water (3 times) to remove any residual salt. The samples were then lyophilized for 3 days to remove traces of water and weighed. Degradation was measured by determining the mass loss of the sample over the period of the study, as shown in equation 2, where $W_o$ represents the initial weight of the specimen and $W_t$ represents its weight after it has been degraded.

$$\text{Mass loss (\%)} = \frac{W_0 - W_t}{W_0} \times 100 \qquad (2)$$

*2.3.8 Statistical Analysis*

Data was expressed as mean ± standard deviation. The statistical significance between two sets of data was calculated using two-tail Student's t-test. Data were taken to be significant, when $p<0.05$ was obtained.

## 2.4 Results and Discussion

### *2.4.1 CUPE Synthesis*

CUPE is a three dimensional thermoset network polymer, synthesized in three steps. The first step involved the bulk polymerization of citric acid with excess 1,8-octanediol to form a low molecular weight, hydroxyl group terminated poly(1,8-octanediol citrate) pre-polymer (pre-POC). The pre-polymer was reacted with 1,6-hexamethyl diisocyanate (HDI) in the second step. Reaction of HDI with the hydroxyl terminated POC resulted in formation of urethane bonds between the pre-POC chains. In this manner, HDI acted as a chain extender to extend the length of aliphatic pre-POC chains to form the longer pre-CUPE chains. Different molar compositions of isocyanates were used in this study to examine the effect of different degrees of chain extension on polymer properties. The still available –COOH and –OH side groups on the pre-CUPE chains would allow further inter-chain polycondensation to obtain crosslinked urethane-doped polyester (CUPE) network via ester bond formation.

### *2.4.2 Infra-Red Analysis*

FT-IR spectra of both, POC and CUPE (Fig 2.2) pre-polymers showed sharp peaks at 1733 $cm^{-1}$, which are characteristic of carbonyl groups on the ester bond. The carbonyl groups of the carboxylic acid side chain of citric acid also contributed to this absorbance. Methylene groups in the polymer chain were represented by the peaks between 2931 $cm^{-1}$ and 2919$cm^{-1}$ in the pre-CUPE and pre-POC spectra [85]. Absorbance from the urethane bonds was observed in the form of a narrow shoulder peak at 3350 $cm^{-}$

[1] in CUPE, while it was absent in POC spectra. Additionally, amide I and amide II vibrations were also observed at 1670 $cm^{-1}$ and 1560 $cm^{-1}$, respectively [67] in CUPE pre-polymers and were absent in the POC pre-polymer spectrum. The presence of these peaks confirmed the incorporation of urethane linkages in the polymer chain. Absence of a peak at 2267 $cm^{-1}$ in the CUPE spectra indicated that all the isocyanate groups had been incorporated in the polymer chains.

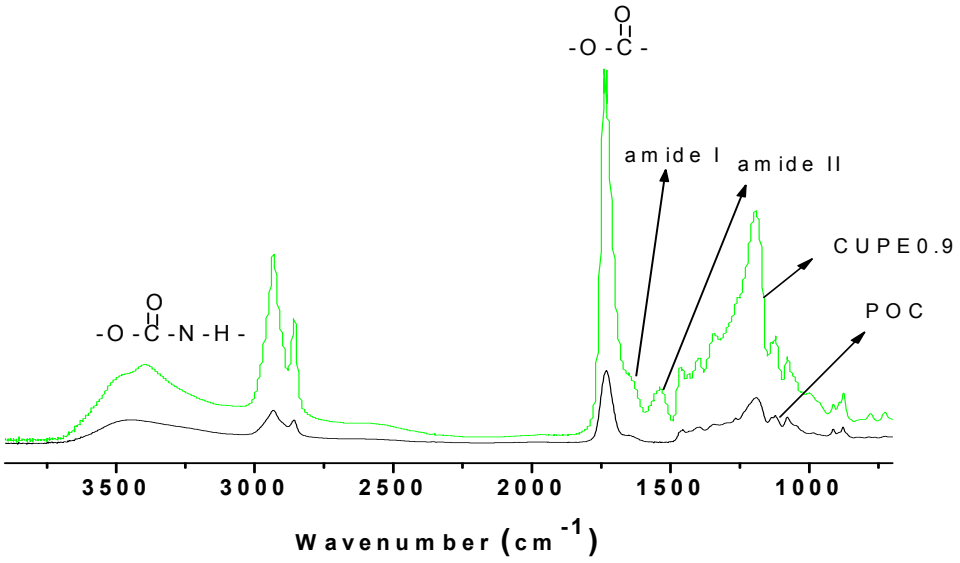


Fig 2.2 FT-IR spectra of a representative crosslinked urethane doped polyester pre-polymer. A. Poly (1,8-octanediol citrate) pre-polymer before chain extension; B. CUPE0.9 pre-polymer after incorporation of urethane bonds.

The effect of post polymerization on CUPE was studied by attenuated total reflectance FTIR (ATR-FTIR) spectroscopy. Fig 2.3 shows the ATR spectra of CUPE0.9 pre-polymer (Sample A) and CUPE0.9 (Sample B, 2 days 80 °C) films. Carbonyl and hydroxyl groups were present in both, the pre-polymer and the crosslinked polymer. This

is advantageous because these free functional groups would allow for the possibility of biofunctionalization if needed.

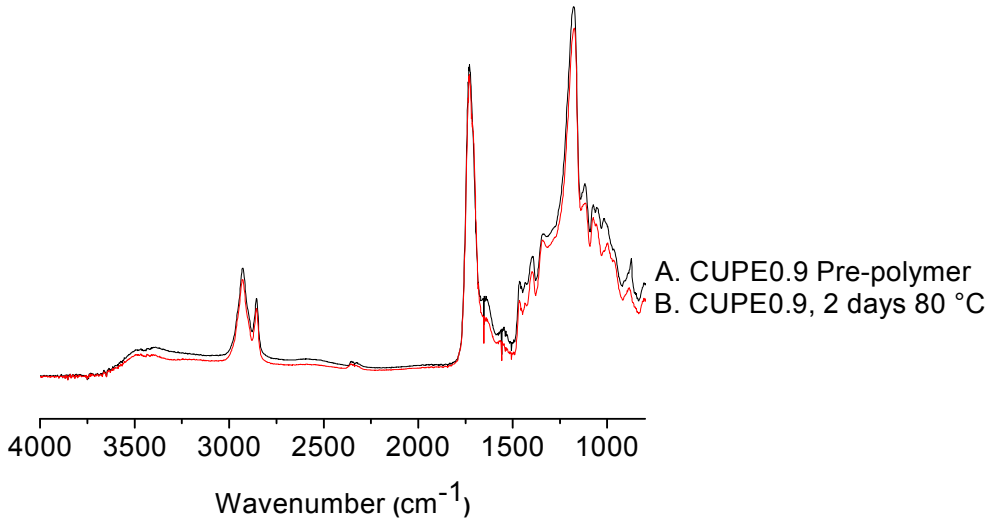


Fig 2.3 ATR spectra of pre-polymer and crosslinked versions of CUPE0.9. The polymerized film was cured at 80 °C for 2 days.

*2.4.3 Thermal Properties*

Thermal properties of the different CUPE polymers were characterized by DSC and TGA. DSC curves (Fig 2.4 a) showed that, under similar polymerization conditions (4 days, 80 °C) the glass transition temperature of CUPEs increased with increasing isocyanate content. The $T_g$ of a polymer is a measure of the ease of chain mobility. In the presence of factors which restrict the movement of the polymer chains, the $T_g$ increases. Typically, polymers with stronger intermolecular forces have more restricted chain mobility and hence, higher glass transition temperatures. CUPE 1.2 had the highest glass transition temperature (Sample C, $T_g$ = 5.20 °C) and CUPE0.6 had the lowest value

(Sample A, $T_g$ = 0.64 °C). The higher $T_g$ of CUPE1.2 is attributed to the larger number of urethane bonds in the backbone of CUPE1.2. The increasing polar urethane bond content would lead to more enhanced hydrogen bonding between the polymer chains. The subsequent decreased chain mobility with increasing isocyanate content would increase the $T_g$ of the higher isocyanate containing CUPEs. All the different CUPE polymers had a higher $T_g$ compared to POC [64], due to the enhanced hydrogen bonding between the polar urethane groups, which are absent in the POC chains. No crystallization or melt peaks were observed for any of the polymers examined, indicating that CUPE was amorphous in nature. Post polymerization conditions were also observed to affect the $T_g$. CUPE1.2 pre-polymer had a lower value of $T_g$ (Sample D, -6.31 °C) compared to the CUPE1.2 sample which had been post polymerized (crosslinked) at 80 °C for four days (sample C). This was attributed to the introduction of ester crosslinks between the polymer chains upon curing. The crosslinks further decreased the chain mobility of the CUPE polymers in comparison to the pre-polymer, leading to a higher Tg value for the polymer.

TGA was used to determine the effect of the isocyanate content on the thermal stability of the CUPE polymers. Results from TGA curves (Fig 2.4 b) indicate that, the thermal stability also increased with increasing the amount of isocyanate in the polymer synthesis. CUPE1.2 was most thermally stable (Sample C, $T_d$ = 322.93 °C), while CUPE0.6 degraded fastest under applied heat (Sample A, $T_d$ = 292.18 °C). This trend may be attributed to the fact that, increasing the isocyanate content used in the synthesis produces higher molecular weight polymers with increased hydrogen bonding between

the urethane groups. Thermal stability of the CUPEs increased with post polymerization due to the presence of stabilizing ester bonds between the polymer chains upon curing. The CUPE1.2 pre-polymer (Sample D, $T_d$ = 270 °C) had a smaller value of $T_d$ compared to post polymerized CUPE1.2 (Sample C, $T_d$ = 322.93 °C).

*2.4.4 Wide Angle X-Ray Diffraction*

X-ray diffraction (XRD) data confirmed the amorphous nature of CUPE. Whereas the PLLA control had well defined and sharp diffraction peaks at 2θ = 17.49 (Fig 2.5 b), CUPE1.2 polymer did not show the presence of any sharp peaks. Instead, a broad peak, which is characteristic of amorphous materials was observed in the XRD spectrum of CUPE (Fig 2.5 a).

*2.4.5 Contact Angle Measurements*

The amount of HDI incorporated into the polymer chain did not affect the initial contact angles of the different CUPE pre-polymers (Fig 2.6). This is likely due to the fact that the urethane bonded segment forms a small portion of the polyester chain and may not greatly influence the wettability of the material. Moreover, the urethane groups which

are inserted into the polymer backbone are polar in nature and would offset the hydrophobicity of the methyl groups in HDI. It was hypothesized that the contact angle of the material was instead determined by the diol that was used during synthesis. This hypothesis was tested by incorporating different molar ratios of Polyethylene glycol (PEG) in the diol segment of the polymer chain. Changing the bulk composition of the

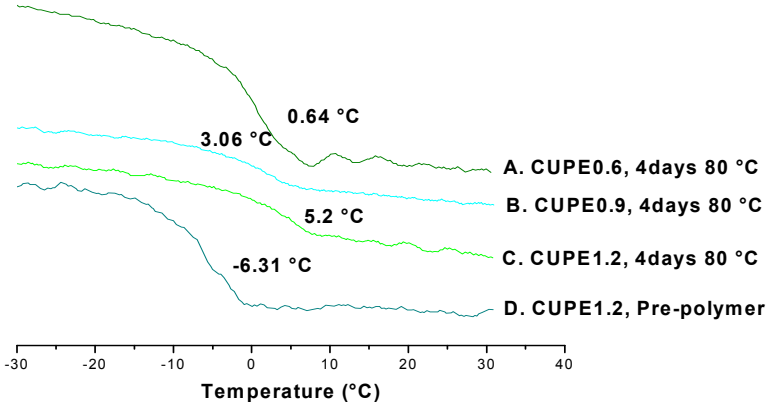


(a)

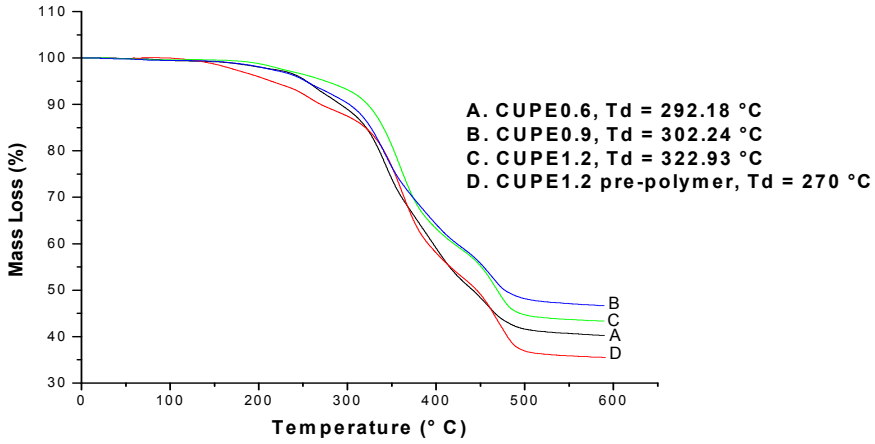


(b)

Fig 2.4 DSC thermograms of CUPEs (a); TGA curves of CUPEs (b); Samples A, B and C correspond to crosslinked CUPEs (80 °C, 4 days) while sample D is a pre-polymer without crosslinks.

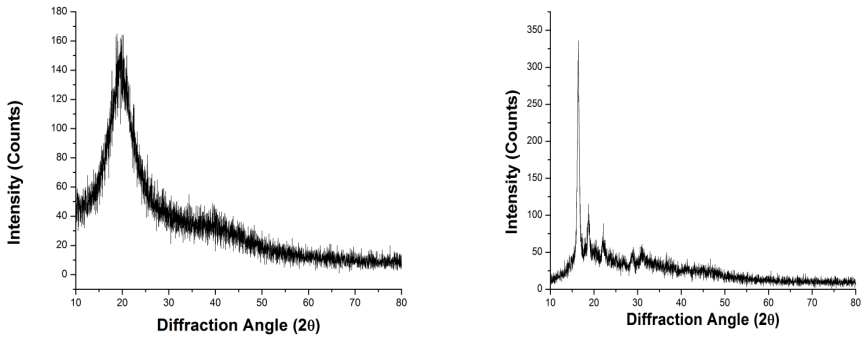


(a) (b)

Fig 2.5 XRD spectra of CUPE (a) showed a broad peak indicating amorphous nature. The sharp peaks of PLLA (b) have been included to discriminate the broad amorphous peaks from the sharp crystalline peaks.

polymer chain by incorporation of more hydrophilic PEG in the diol segment reduced the initial contact angle. CA-PEGU0/1 showed the smallest initial contact angle (42.78 °±1.51°), because of the bulk PEG in the polymer chain (Fig 2.6). CUPE with 1,8-octanediol was most hydrophobic (94.20°±2.87°) due to the presence of the 8 methyl groups of octane-diol in the chain. The initial contact angle increased when some portion of or all the PEG was replaced with the relatively more hydrophobic 1.8-octanediol.

*2.4.6 Mechanical Properties*

The load bearing capability of a tissue engineering scaffold often governs its utility for in vivo applications. In addition to matching the mechanical properties of the target tissue for effective functionality, the scaffolds must be strong enough for surgical handling as well. From the results obtained, it could be seen that the mechanical properties of CUPE could be modified by varying three different parameters; (a) Choice of diol (data not

shown) (b) choice of isocyanate and its molar ratio used during synthesis and (c) post polymerization conditions. Additionally, the stress strain curves of CUPE were characteristic of elastomers (Fig 2.7a). The tensile strength was observed to increase with increasing the isocyanate composition during synthesis. CUPE1.2 had the highest break stress (41.07±6.85 MPa), while CUPE0.6 had the least tensile stress at break (14.6±1.004 MPa). There was no significant difference in the break elongation of the different CUPE

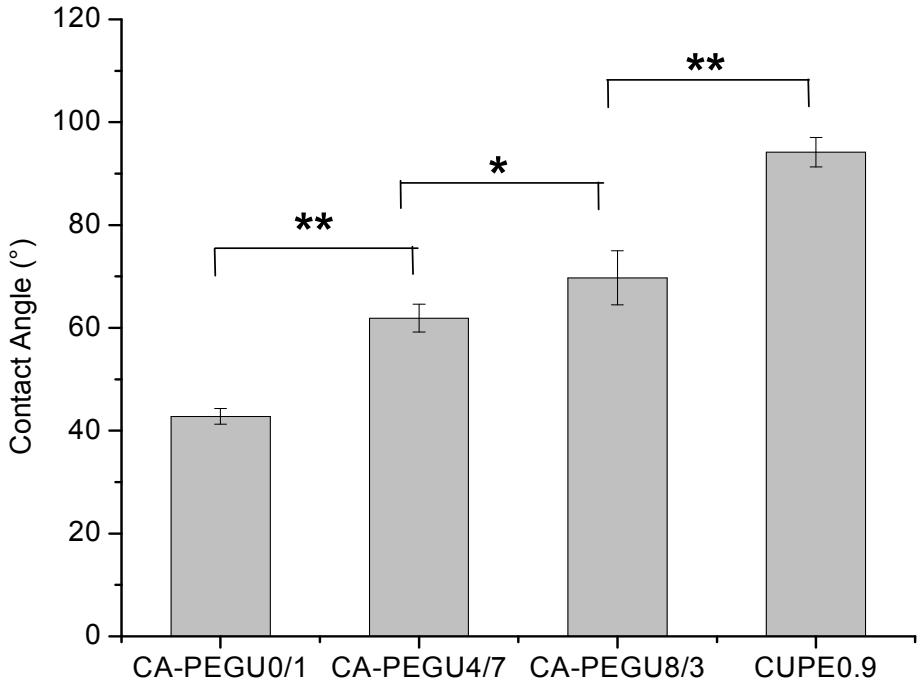


Fig 2.6 Initial contact angles of the different CUPE pre-polymers. Readings were taken for each specimen and averaged (N = 8). Contact angle was observed to decrease with increasing the ratio of hydrophilic PEG in the polymer backbone. * corresponds to $p<0.05$, ** represents $p<0.01$.

polymers. Initial modulus of the different polymers ranged from 4.14±1.71 MPa to 38.35±4.49 MPa. The effect of polymerization conditions on the mechanical properties was also investigated. Increasing the post polymerization time and temperature was

observed to increase polymer tensile strength with a corresponding decrease in polymer elongation at break (Fig 2.7 b,c).

CUPE demonstrates greater flexibility compared to poly(diol citrates) in producing constructs with tunable mechanical properties. Although the mechanical properties of both, poly(diol citrates) and CUPE may be varied by varying the choice of diol used in the synthesis and the duration of crosslinking, CUPE can produce a wider range of properties by variation of the isocyanate content and composition. Since the mechanical properties of a scaffold are directly related to that of the polymer used to fabricate it, CUPE could be used to make scaffolds with varying mechanical properties required for a more diverse range of tissue engineering applications as opposed to poly(diol citrates). Moreover, the tensile strength of CUPE1.2 was 20 times greater than that of its precursor, poly(octane diol) citrate. The high load bearing abilities of CUPE may be exploited for the engineering of dynamically active tissues like ligaments and tendons which is not possible with poly(octane diol) citrates.

### *2.4.7 Density and Molecular Weight between Crosslinks ($M_c$)*

Among the different CUPE compositions tested, CUPE1.2 had the lowest density (1.1717±0.0211 g/cm3), while CUPE0.6 was the most dense (1.2253±0.0207 g/cm3) (Table 2.1). A similar trend could also be observed for the molecular weight between crosslinks for the different CUPE polymers tested. CUPE1.2 and CUPE0.6 had the lowest and highest values of $M_c$ respectively. The significantly lower density of CUPE1.2 could be explained by the incorporation of diisocyanate and subsequent participation of

urethane bonds as inter chain crosslinks. Under reaction conditions excess diisocyanate in the reaction mixture would be forced to react with the hydroxyl and carboxyl pendant groups of the citric acid monomer forming urethane bonds and amide bonds, respectively. The incorporation of a long chain (in this case, 6 carbon chain) crosslinks between the polymer molecules would increase the inter chain volume and subsequently result in reduced density.

Table 2.1 Density measurements, Mechanical properties and crosslink densities of different CUPE polymers. Polymerization conditions were 80 °C treatment for 2 days, unless otherwise specified.

| **Sample** | **Density ($g/cm^3$)** | **Young's Modulus (MPa)** | **Tensile Strength (MPa)** | **Elongation (%)** | ***n*** **($mol/m^3$)** | **$M_c$ (g/mol)** |
|---|---|---|---|---|---|---|
| CUPE0.6 | 1.2253±0.0207 | 2.99±0.53 | 16.02±2.39 | 252.37±35.12 | 402±71 | 3125 ±588 |
| CUPE0.9 | 1.2008±0.0541 | 5.84±1.84 | 32.10±2.69 | 278.24±10.12 | 786±248 | 1637±404 |
| CUPE1.2 | 1.1717±0.0211 | 29.82±2.67 | 33.35±3.26 | 260.87±22.22 | 4012±359 | 294±27 |
| CUPE1.2, 1d 80 °C | 1.1944±0.0155 | 4.84±0.90 | 28.75±1.28 | 265.43±26`.144 | 651±121 | 1885±316 |
| CUPE0.6, 1d 80 °C | 1.2114±0.0168 | 2.53±0.30 | 15.62±2.75 | 291.26±17.90 | 341±40 | 3589±406 |

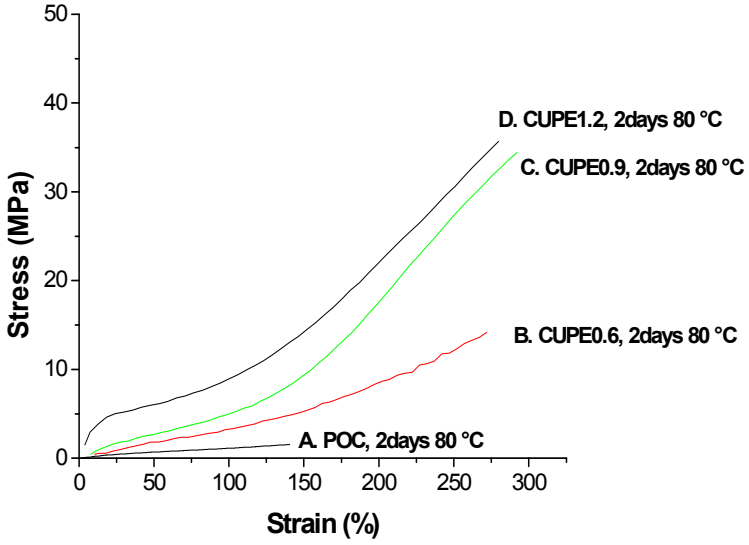


(a)

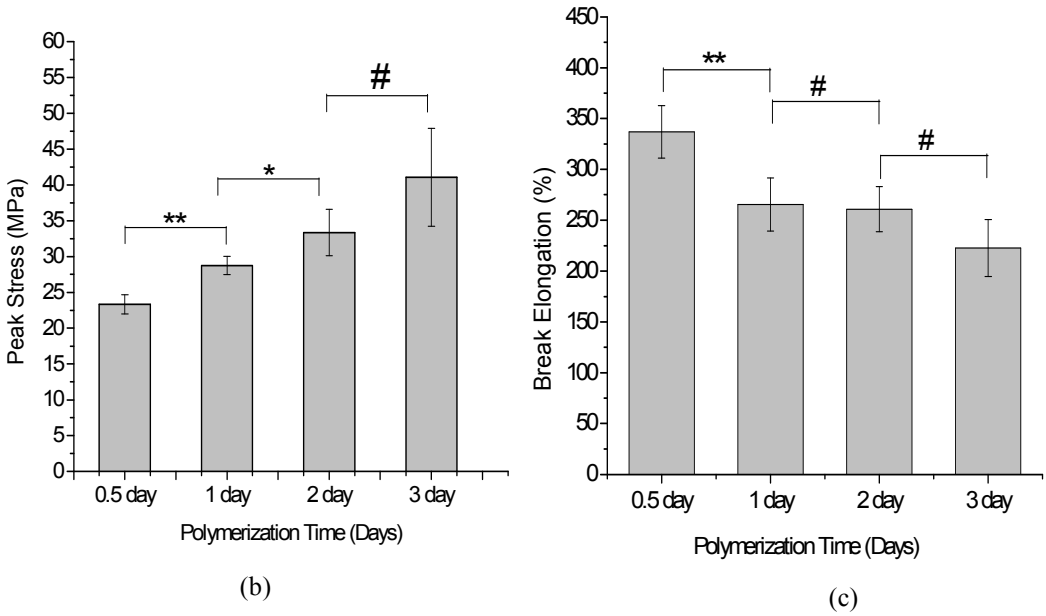


(b) (c)

Fig 2.7 Tensile stress-strain curves of the different CUPE polymers and crosslinked POC polymer. All the polymers shown were polymerized at 80 °C for 2 days (a). Effect of post polymerization conditions on the peak stress (b), and elongation at break (c) are shown. ** corresponds to $p<0.01$, * denotes $p<0.05$. N = 5.

*2.4.8 In Vitro Degradation*

Degradation profiles of the different polymers are presented in Figure 2.8. Polymers with higher isocyanate content exhibited faster degradation rates in both PBS and NaOH. CUPE1.2 demonstrated a mass loss of 16%±0.32% after two months in PBS, while CUPE0.6 lost only 8.13%±2.04% of its initial mass under similar conditions (Fig 2.8a). This result was interesting, because CUPE1.2 had the highest degree of crosslinking in all the different CUPE polymers tested. This phenomenon however, may be explained by the lower density and consequently larger inter-chain volume of CUPE1.2 (Table 2.1). A higher inter-chain volume would permit greater access to the hydrolytically labile ester bonds in the crosslinks and the polymer backbone, leading to a faster degradation rate of the polymer. Increasing the polymerization time also made the CUPE polymers more resistant to degradation due to the introduction of more ester crosslinks between the polymer chain upon curing (Fig 2.8b). Additionally, the degradation rate was observed to be a function of the choice of diol used in the synthesis as well. Increasing the hydrophilicity of the diol used in the synthesis resulted in faster degradation rates as evidenced by the faster rate of degradation of the CUPE polymers containing poly(ethylene glycol) (PEG) in different ratios (Fig. 2.8c).

In addition to load bearing abilities, the rate of regeneration of different tissues also vary. As with mechanical properties, CUPE offers a much wider range of degradation rates compared to poly (diol citrates) owing to variations in the degree of isocyanate addition and composition.

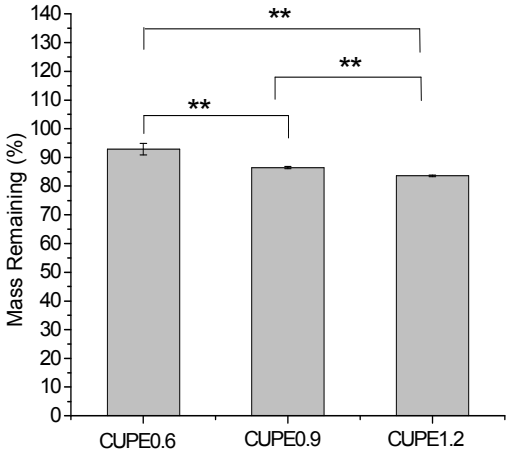


(a)

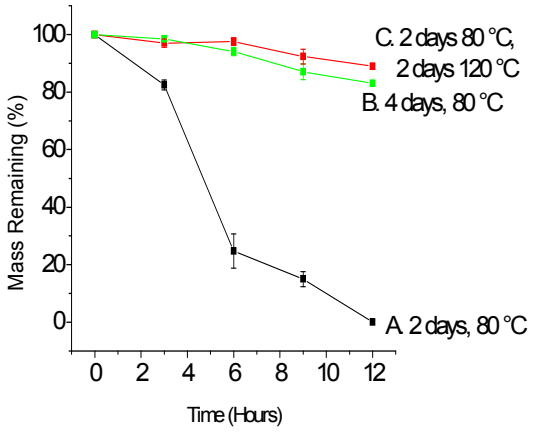


(b)

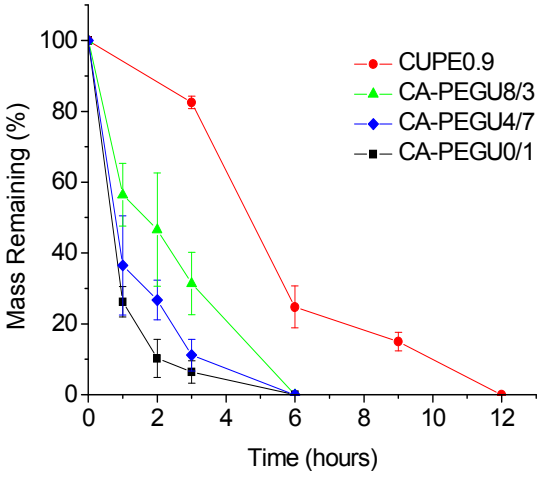


(c)

Fig 2.8 Degradation studies of CUPE in (a) PBS at 37 °C (n=6) for 8 weeks and (b),(c) 0.05M NaOH solution at room temperature. The different polymers used in the PBS degradation study were polymerized at 80 °C for 2 days (a). CUPE0.9 polymer was used to study the effect of different post polymerization conditions on the degradation rate of CUPEs (b). Effect of diol composition used for CUPE synthesis on degradation profiles was also studied. (c). ** corresponds to $p<0.01$. N = 5.

## 2.5 Conclusion

In this set of studies, the effect of isocyanate content on the properties of crosslinked urethane doped polyesters (CUPEs) was analyzed. Spectral analysis confirmed the incorporation of the urethane bonds into the polymer chain. Irrespective of the isocyanate content, the polymer remained amorphous as indicated by DSC and XRD data. Contact angle measurements indicated variation in the isocyanate content did not affect the surface hydrophilicity of the material, whereas changing the bulk properties of the material by using more hydrophilic diols made the material hydrophilic. Three different parameters were found to affect the rate of degradation of the polymer namely, the choice of diol, polymerization conditions and the isocyanate content. Finally, CUPE demonstrated a twenty fold increase in the mechanical properties compared to its pre-cursor POC, while preserving nearly the same degree of elasticity. These results indicate that CUPE may be able to produce stronger and more suturable scaffolds. The versatility offered by CUPE in the control of its mechanical properties and degradation rates, may be exploited to design grafts which match the properties of native vasculature, thus improving compliance of the grafts.

# CHAPTER 3

# EVALUATION OF *IN-VITRO* AND *IN-VIVO* BIOCOMPATIBILITY OF CUPE

## 3.1 Introduction

Both poly(diol citrates) and biodegradable polyester-urethanes have been demonstrated to be biocompatible in various studies [17, 64-66, 68, 76]. Biocompatibility evaluation of CUPE was necessary to determine if the introduction of the urethane bonds into the polyester network, adversely affected its biocompatibility. In vitro studies were performed to determine the ability of CUPE to support cell growth and proliferation. In vivo studies were conducted in order to determine the degree of host response elicited by CUPE.

## 3.2 Materials and Methods

### *3.2.1 Materials*

All cell culture media and supplements were obtained from Atlanta Biologicals (Carlsbad, CA), whereas serum was purchased from HyClone (Logan, UT). LIVE/DEAD Viability/Cytotoxicity Kit was purchased from Invitrogen (Carlsbad, CA).

*3.2.2 3T3 Fibroblast and Human Aortic Smooth Muscle Cell Culture*

NIH 3T3 fibroblast cells (FCs) and human aortic smooth muscle cells (HASMCs) were cultured in 75 $cm^2$ tissue culture flasks with Dulbecco's modified eagle's medium (DMEM), which had been supplemented with 10% fetal bovine serum (FBS) and 1% penicillin-streptomycin. Cells were incubated in a humid environment at 37 °C and 5% $CO_2$. HASMCs were not used beyond passage 10. The cells were cultured to 90% confluency after which they were either passaged or used in experiments.

*3.2.3 Cell Seeding on CUPE films*

CUPE1.2 was used for all cell culture studies. Cells were seeded on CUPE films which had been prepared as mentioned earlier. The films were cut into discs of 7 mm diameter using a cork borer and sterilized by treatment with 70% ethanol for 30 minutes, followed by another 30 minutes of UV light exposure. The sterilized samples were leached in sterile PBS to remove excess ethanol and then immersed in complete media for 24 hours prior to seeding. The cells were trypsinized, centrifuged and suspended in media to obtain a seeding density of $3x10^5$ cell/ml for the films. 200 µl of the cell suspension was added on top of the polymer specimens in the culture dishes. After 1 hour of incubation at 37 °C, 5 ml of media was added to each culture dish. After 3 days and 6 days in culture for the films and scaffolds respectively, the cells were fixed by addition of 5 ml of 2.5% (wt/v) gluteraldehyde-PBS solution. Qualitative examination of the cell morphology on the films and scaffolds was performed using scanning electron microscopy (SEM, Hitachi 3500N SEM). Briefly, the fixed film and scaffold specimens

were sequentially dehydrated by treatment with a graded series of ethanol (50, 75, 95, and 100%), freeze dried and then sputter coated with silver. SEM images at different magnifications were obtained. Cell seeded scaffolds were also stained using a live dead assay kit (LIVE/DEAD Viability/Cytotoxicity Kit, Invitrogen, Carlsbad, CA) and observed under a fluorescence microscope.

*3.2.4 Cell Growth and Proliferation on CUPE films*

A quantitative assessment of cell growth and proliferation on CUPE films was performed using the Methylthiazoletetrazolium (MTT) cell proliferation and viability assay. The ability of CUPE to promote attachment, growth and proliferation was evaluated in comparison to PLLA relative control using HASMCs as the model cell line. On basis of results obtained in the qualitative study, CUPE1.2 films were chosen as the representative CUPE material and were prepared as per earlier mentioned methods. PLLA films were prepared by casting 10 ml of a 3% solution of PLLA in chloroform, into a Teflon mold. The Teflon mold was placed in a chemical hood equipped with laminar air flow to allow solvent evaporation. As per the above cell seeding procedure, the CUPE and PLLA discs were sterilized, leached in media and seeded with 5000 cells each and allowed to grow and proliferate for the respective time points. The old media was replaced with fresh complete media on a daily basis throughout the duration of the study. Three time points were used for the MTT Assay analysis (1, 3, and 5 days). At the end of each time point, the assay was performed as per the manufacturer's protocol. Briefly, the old media was aspirated, and each specimen was thoroughly washed 3 times with PBS to remove any loosely attached cells and dead cells. 100 µl of incomplete

media (DMEM without serum) was added to these specimens. 10 µl of 3-(4,5-dimethylthiazol-2yl)-diphenyltetrazolium bromide solution was then added to the wells containing the cells and the blanks, and they were incubated at 37 °C for 3 hours. At the end of incubation period, the mixture of the MTT solution and incomplete media was aspirated and replaced with 100 µl of MTT solvent. Dissolution of formazan crystals was facilitated by constantly agitating the well plate on an orbital shaker for 15 minutes. Absorbance was analyzed with an Infinite200 microplate reader (Tecan Group Ltd., Switzerland) at 570 nm, with a reference wavelength of 690 nm, within 30 minutes of MTT solvent addition.

*3.2.5 Evaluation of Foreign Body Response to CUPE*

CUPE1.2 was chosen as the representative polymer to evaluate the response elicited by the polymer in an *in vivo* implantation. Both films and salt leached scaffold forms of CUPE and PLLA samples (as relative control) were used in this experiment. The films and scaffolds were cut into discs (10 mm diameter, and 1 mm thickness) and, then implanted subcutaneously in the back of healthy, female Sprague Dawley rats (Harlan Sprague Dawley, Inc., Indianapolis, IN). Animals were cared for in compliance with regulations of the animal care and use committee of University of Texas at Arlington. Briefly, the discs were first sterilized by treatment with 75% ethanol for 30 minutes followed by treatment under UV light for another 30 minutes. 25 SD rats were divided into groups of 5 rats each for the different time points of the study. The rats were anesthetized in a chamber through which an isofluorane-oxygen mixture was passed. Test samples were randomly implanted in upper or lower part of the back of the rats by blunt

dissection. At the end of each time point, the rats were sacrificed and the implant and surrounding tissue were frozen in OCT embedding media (Polysciences Inc., Warrington, PA) at -80 °C for histological analyses. To assess the tissue responses to film and scaffold implants, tissue sections were hematoxylin & eosin (H&E) stained. Images of stained sections were taken at 10 x magnifications using a Leica DMLP microscope fitted with a Nikon E500 camera (Nikon Corp. Japan). Three different non overlapping images per section were collected for analysis. Fibrous capsule thickness was measured in each of the images using the line tool in ImageJ analysis software. Atleast 25 readings from different parts of the images were collected and averaged to determine the capsule thickness.

### *3.2.6 Statistical Analysis*

Analysis of the results was performed using two tail student's t-tests with $p<0.05$ being considered as being significant. All results were presented as mean ± standard deviation (SD).

## 3.3 Results and Discussion

NIH 3T3 fibroblasts and HASMCs were seeded on CUPE films. Under SEM observation, it could be seen that the cells attached and proliferated over the surface of the films. Both cell types displayed normal phenotype and grew to confluence over a 3 day period (Fig 3.1). No pre-treatment or pre-coating of CUPE films was required to facilitate the cellular attachment and growth.

In addition to a qualitative assessment, cell adhesion and proliferation was also quantitatively evaluated using the MTT assay. Results indicated that initially (at day 1 and day 3) a larger number of cells attached to the CUPE surface compared to PLLA control films (Fig 3.2). Cells continued to proliferate and increased in number over the 1 week study period, wherein, both CUPE and PLLA had comparable cell numbers.

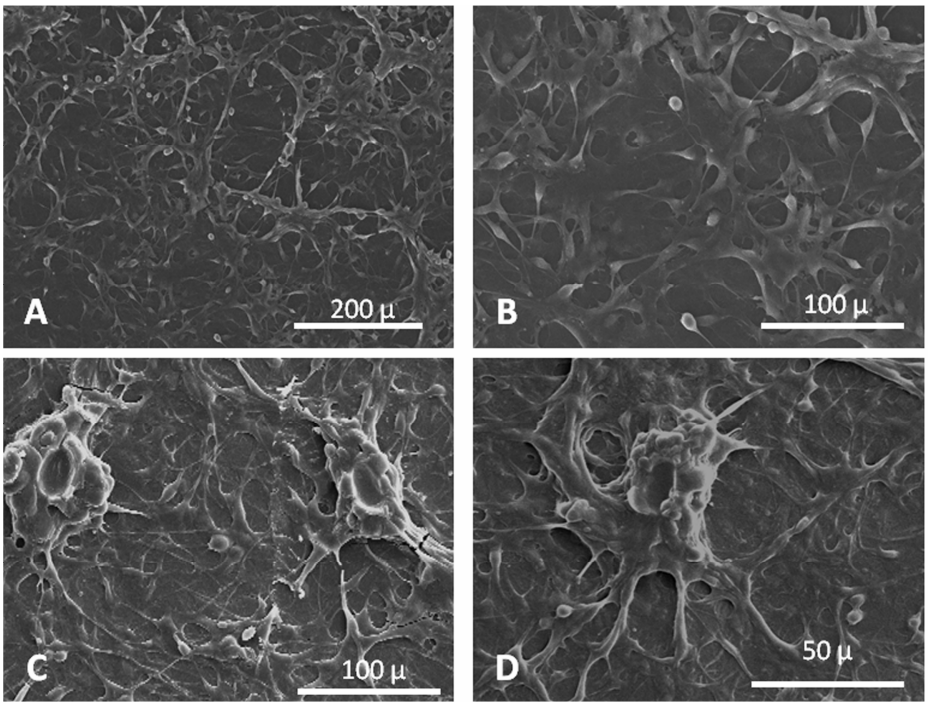


Fig 3.1 SEM images of HASMCs (A, B) and fibroblasts (C, D) growing on the surface of CUPE1.2 films after three days in culture. Seeding density of $3x10^5$ cells were used per film (7 mm diameter).

The foreign body response to CUPE was studied by subcutaneous implantation of CUPE films and scaffolds in Sprague Dawley rats. Both CUPE and PLLA implants were

surrounded by well defined fibrous capsules at both, 1 week and 4 week time points (Figure 3.3). Additionally, no necrotic tissues were found on both CUPE and PLLA implants at both time points. The fibrous capsules surrounding the CUPE implants (Film: 245.3±13.46 microns; Scaffold: 436.6±29.42 microns) (Fig 3.3 A, B) were substantially thinner than those surrounding the PLLA implants (Film: 314.23±17.48 microns, $p<0.001$ compared to CUPE film; Scaffold: 584.63±49.83, $p<0.001$ compared to CUPE scaffold) (Fig 3.3 C, D) at the 1 week time point. There was a significant reduction of 28% and

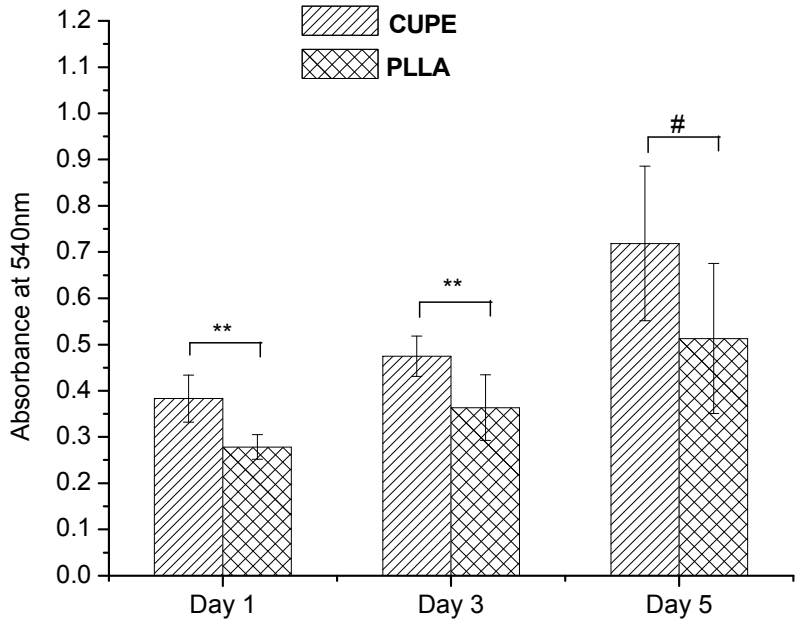


Fig 3.2 Comparison of growth rate of HASMCs on PLLA (control) and CUPE films. MTT absorption was measured at 570 nm. N = 6. ** corresponds to $p<0.01$ and # represents $p>0.05$

58% in the thickness of the fibrous capsules surrounding the PLLA films and scaffolds, respectively, (Fig 3.3 G, H) at 4 weeks. Capsule thickness was comparable for both

CUPE and PLLA implants at 4 weeks. These results suggest that CUPE implants incited weaker acute inflammatory responses than PLLA implants. Furthermore, the extent of chronic tissue responses, to CUPE and PLLA are very similar. The weaker acute inflammatory response coupled with the similar chronic inflammatory response, suggests that CUPE may be less pro-inflammatory compared to PLLA.

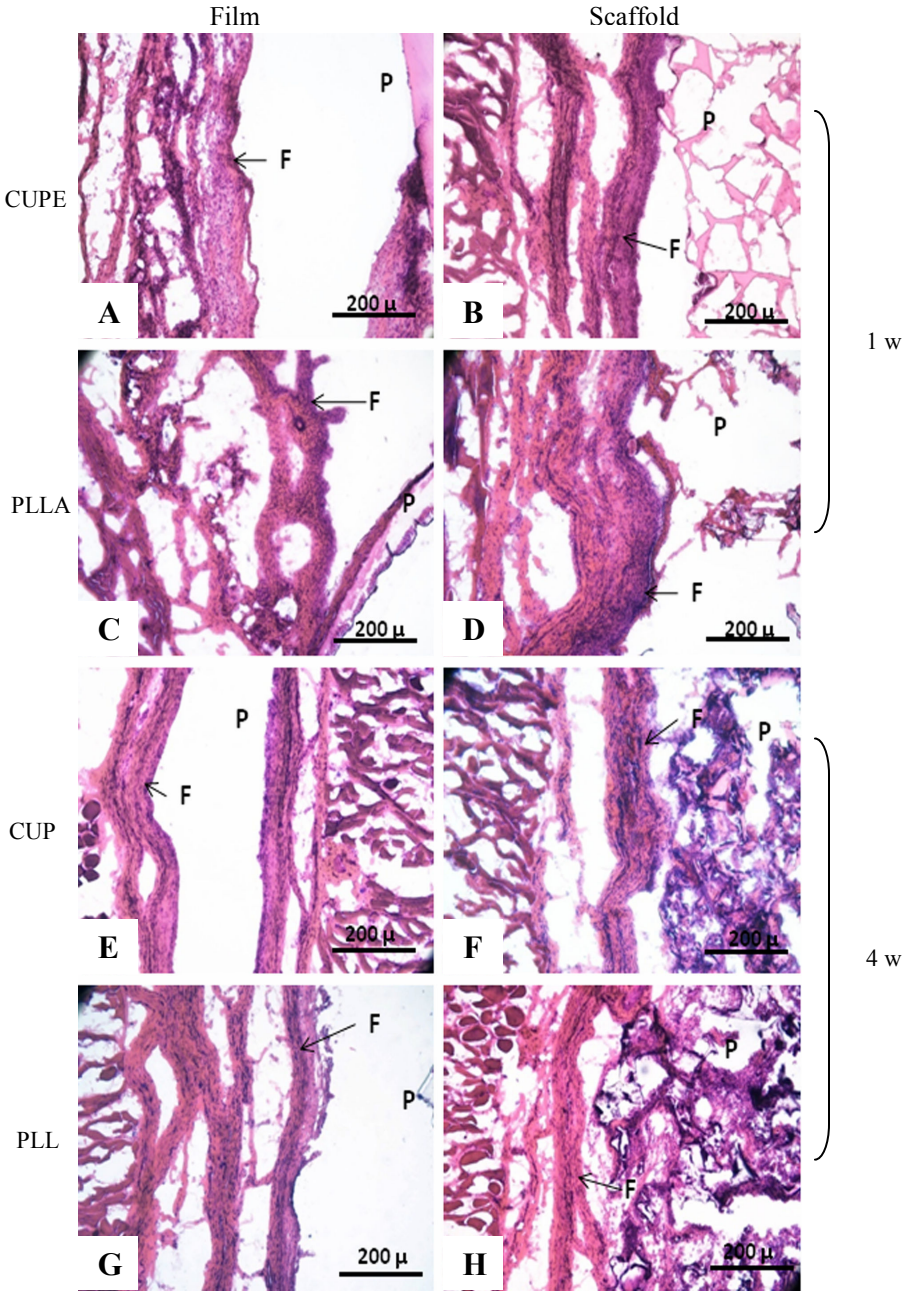


Fig 3.3 Histology of in vivo response to CUPE1.2 film (A,E) and salt leached scaffold discs (B,F). PLLA films (C,G) and scaffolds (D,H) served as control. P and F are used to indicate the regions of polymer and fibrous capsule respectively. All images were taken at 10x magnification. On the 1 week samples, although all samples were covered by a well defined fibrous capsule, CUPE implants were consistently surrounded by a thinner fibrous capsule as opposed to PLLA implants. In the case of the 4 week implants, overall, all the implants appear to yield similar extent of tissue response.

## 3.4 Conclusion

This set of studies was aimed at exploring the cell-material interactions of CUPE to determine its suitability as a tissue engineering material. The cell lines tested were observed to proliferate on the material surface, while maintaining normal phenotype. The results also indicated that the rate of cell growth was comparable and at some points better than another commonly used degradable polymer – PLLA. Additionally, CUPE films and scaffolds were less pro-inflammatory in an in vivo environment in comparison to PLLA. These results indicate that CUPE is a comparable or better substrate than PLLA for cell growth and proliferation. These results are indicative of CUPE as a suitable material for tissue engineering.

# CHAPTER 4

# HEMOCOMPATIBILITY EVALUATION OF CUPE

## 4.1 Introduction

Materials designed for blood contacting applications should not have adverse effects on circulating blood components. These include circulating platelets and leukocytes in particular, since these components are responsible for initiating adverse physiological responses like thrombus formation, initiation of the coagulation cascade or an acute inflammatory response [86]. Various techniques have been used to either mitigate or avoid these adverse responses. These include using coatings of anti-coagulants like heparin or hirudin [87], immobilization of polyethylene glycol [88] and use of anti-platelet agents like dipyridamole [89]. The hemocompatibility of CUPE was tested in order to evaluate its potential application as a vascular graft material. Parameters tested included platelet adhesion and activation, leukocyte activation, whole blood clotting time and hemolysis.

## 4.2 Materials and Methods

### *4.2.1 Materials*

LDH-Cytotoxicity assay kits were purchased from Biodivision Inc. (Mountain View, CA). Reagents for flow cytometry analysis including CD42a R-phycoerythrin (R-PE)-conjugated mouse anti-human monoclonal antibodies, CD62p allophycocyanin (APC)-conjugated mouse anti-human monoclonal antibodies, CD45 APC-conjugated

mouse anti-human monoclonal antibodies, CD 11b/Mac-1 PE-conjugated mouse anti-human monoclonal antibodies, Human TNF and IL-1β Cytometric Bead Array (CBA) were purchased from Becton Dickinson Biosciences, San Jose, CA. All chemicals were purchased from Sigma-Aldrich (St. Louis, MO), and used as received unless otherwise specified. Dulbecco's Phosphate-Buffered Saline (PBS, pH=7.4) was purchased from Invitrogen (Carlsbad, CA). Gluteraldehyde buffer had 2.5% (w/v) gluteraldehyde in PBS, pH=7.4. Triton-PSB buffer contained 2% (v/v) Triton X-100 in PBS, pH=7.4.

*4.2.2 Preparation of Platelet Rich Plasma (PRP)*

All methods related to collection and handling of whole blood and blood components like plasma and platelets were approved by the Institutional Review Board at the University of Texas at Arlington. Acid citrate dextrose (ACD) anticoagulant containing tubes were used to collect blood drawn from healthy individuals by venipuncture. PRP was prepared using methods previously described in literature [69]. Briefly, whole blood was centrifuged at 250g for 15 minutes to separate the blood components. Using a sterile transfer pipette, the clear supernatant containing the PRP was collected for platelet adhesion studies.

*4.2.3 Platelet Adhesion*

Platelet adhesion to the different polymer surfaces was examined by scanning electron microscopy (SEM) (Hitachi S3000N). 200 µl of PRP was added on top of the PLLA and CUPE discs. After 1 hour of incubation at 37°C, PRP was aspirated and the

samples were rinsed thoroughly with PBS 3 times to remove any loosely adhered and unattached platelets. The adhered platelets were fixed using 2.5% gluteraldehyde-PBS solution, sequentially dehydrated in a graded series of alcohol (50%, 75%, 90% and 100%) and lyophilized. The samples were sputter coated with silver and examined using SEM. 3 specimen discs of each polymer were prepared for SEM observation.

Quantitative assessment of adherent platelets was evaluated using the lactate dehydrogenase (LDH) assay as previously described [69, 90]. Polymer samples were incubated and washed per the aforementioned procedure for SEM sample preparation. The samples were then treated with 2% Triton-PBS buffer for 30 minutes at 37°C to lyse the adhered platelets. 100 µl LDH Assay substrate was added to the platelet lysate and incubated for 30 minutes at 37 °C in darkness. 0.1 N HCl was added to stop the reaction at the end of the incubation period. Optical density was measured at 490 nm with a reference wavelength of 650 nm.

*4.2.4 Platelet Activation*

Platelet activation was assessed by measuring the expression of P-selectin on platelet plasma membrane [86, 91]. Briefly, CUPE, PLLA, and TCP samples were treated with 200 µl of PRP for 1 h at 37 °C. 5 µl of the material exposed PRP was incubated with 20 µl phycoerythrin (PE)-conjugated mouse anti-human CD42a monoclonal antibodies and 20 µl allophycocyanin (APC)-conjugated mouse anti-human CD62p monoclonal antibodies at room temperature for 30 minutes in darkness. CD42a, known as platelet glycoprotein IX (GP9), is a small membrane glycoprotein found on the

platelet plasma membrane, and is used as a platelet marker. CD62p, a member of the P-selectin family, is used as an indicator of activated platelets. After staining, the cells were fixed with 1% paraformaldehyde and measured for the antibodies bound to platelet membranes using FACSarray bioanalyzer (Becton Dickinson FACSArray, San Jose, CA). 10,000 platelets were acquired and the mean values of red fluorescence intensity (APC-CD62p), which corresponds to the activation of platelets, were measured. These values were compared with that of the PLLA group, which was set to 100% as the control.

*4.2.5 Whole Blood Clotting Time*

Kinetic whole blood clotting time was used to evaluate the thromboresistant properties of CUPE [92, 93]. Briefly, 850 µl $CaCl_2$ (0.1 M) was added to 8.5 ml ACD blood to initiate the clotting reaction. 100 µl re-calcified blood was immediately added on top of CUPE, PLLA, TCP and glass discs and incubated at room temperature for 10, 30, and 60 minutes. At the end of incubation time, the samples were treated with 3 ml of DI water for 5 minutes to lyse the unclotted red blood cells. The hemoglobin released from lysed red blood was measured at 540 nm absorbance using a microplate reader (Infinite M200, Tecan, Switzerland). The absorbance values were plotted versus the blood contacting time.

*4.2.6 Leukocyte Activation*

The activation of leukocytes was also measured by flow cytometry. 100 µl whole blood was incubated with CUPE, PLLA, or TCP samples for 1 h at 37°C. Following incubation, the whole blood samples were treated with 10 µl APC-conjugated mouse anti-human CD45 monoclonal antibodies and 20 µl PE-conjugated mouse anti-human CD11b monoclonal antibodies for 30 minutes at room temperature in darkness. CD45 is the leukocyte maker while CD11b is used as an activated leukocytes maker. The red blood cells in the whole blood were lysed using 1× FACS lysing solution. The antibodies conjugated leukocytes were fixed with 1% paraformaldehyde and analyzed with FACSarray bioanalyzer. 5,000 leukocytes were acquired and their mean values of yellow fluorescence density (PE), corresponding to CD11b were calculated. These values were compared with that from the PLLA group, which is set to 100% as a control group.

*4.2.7 Inflammatory Cytokine Release*

The inflammatory cytokines IL-1β and TNF- α were measured using Cytometric Bead Array (CBA). Briefly, CUPE, PLLA and TCP samples were treated with 100 µl whole blood for 1 h at 37°C. After incubation, the blood was collected and centrifuged at 2000 g for 10 minutes. The supernatant was carefully aspirated to obtain the platelet poor plasma (PPP). Concentrations of released IL-1β and TNF-α in the PPP were measured using Human TNF Flex Set and Human IL-1β Flex Set (Becton Dickinson Biosciences, San Jose, CA) following the manufacturer's instructions. Briefly, two single bead populations with distinct fluorescence intensity and capture antibodies against IL-1β or TNF-α were

incubated with the PPP samples. The bead population was resolvable in the FACSarray bioanalyzer based on their position. PE-conjugated antibodies against IL-1β or TNF-α were further incubated with the beads and analyzed with FACSarray bioanalyzer. IL-1β and TNF-α standards with known concentrations were measured for calibration. The concentration of IL-1β and TNF-α were calculated based on the yellow fluorescence intensity (PE) and the bead numbers using the software provided with the assay.

*4.2.8 Hemolysis*

The percentage of biomaterial-mediated hemolysis is quantified using an established method [69, 94]. 200 µl of fresh ACD blood was diluted in 10 ml 0.9% saline. 200 µL diluted blood was incubated with each polymer sample for two hours at 37°C under gentle agitation. 0.9% saline diluted blood without polymer contact served as negative controls (NC), and 200 µl whole blood diluted with DI water served as positive control (PC). After incubation, the polymer samples (PS) were carefully removed and the blood samples were centrifuged at 1000 g for 10 min. The supernatant was transferred to a 96 well plate and the absorbance (Abs) was measured at 545 nm. Percentage hemolysis was calculated for each polymer using the following equation.

$$\%Hemolysis = \frac{Abs_{PS} - Abs_{NC}}{Abs_{PC}} \times 100 \qquad (1)$$

*4.2.9 Statistical Analysis*

All results were presented as mean ± standard deviation. Statistical significance between data sets was established with two-tail Student's t-test. A p value $<0.05$ was considered to be significant.

## 4.3 Results and Discussion

*4.3.1 Platelet Adhesion*

Contact activated thrombosis is one of the primary causes for failure of blood contacting devices like arterial stents and synthetic vascular grafts [54, 95]. Blood contact causes the irreversible adsorption of various pro-coagulant plasma proteins on the biomaterial surface. Upon adsorption, soluble plasma proteins undergo a conformational change which exposes active epitopes. Receptors of circulating platelets bind to these epitopes and cause surface adhesion and subsequent activation of the platelets. Platelets may adhere to the surface via passive binding or active binding. Passive binding to the surface occurs without consequent activation, while an active binding is accompanied by morphological changes and release of various active pro-coagulant biomolecules [86]. Our results showed that platelets adhered to both CUPE (Fig. 4.1a and 4.1b) and PLLA (Fig 4.1c and 4.1d). However, there was a distinct difference in morphology of the adhered platelets. Platelets on CUPE were mostly round without any cytoplasmic extensions. This indicates that even though platelets adhere to CUPE, they do not undergo significant morphological changes (Fig. 4.1a, 4.1b). On the other hand, majority of the platelets on PLLA discs were in the spread dendritic phase, a morphology, which is

characterized by flattened platelets (Fig. 4.1c, 4.1d) with extensive pseudopodial processes. This extent morphology of platelets has been demonstrated as an indicator of platelet activation [96]. The LDH assay was used to quantify adhered platelet numbers on PLLA and CUPE surfaces. This method of co-relating observed lactate dehydrogenase activity to number of adhered platelets was first proposed by Tamada et al. [97] and has been subsequently used in previous researches [69, 90, 98, 99]. Compared to PLLA, there was a 39% reduction in the number of platelets adhered to CUPE of the same surface area (Fig. 4.2).

*4.3.2 Platelet Activation*

Studies have shown that although the materials may not support significant platelet adhesion, they may potentially still activate platelets [100, 101]. Therefore, to better assess the interaction of a material with platelets, the degree of platelet activation must also be investigated. P-selectin is a glycoprotein which is stored in cytosolic α-granules in resting platelets. Upon activation, the granular contents are released and P-selectin is translocated to the platelet membrane where it mediates platelet-platelet and platelet-leukocyte interactions [86, 91]. Since membrane bound P-selectin is expressed only on activated platelets, it can be used as a marker to measure the relative activation of platelets by different biomaterials [102, 103]. As shown in Figure 4.3, the results showed that activation degree of the platelets exposed to CUPE is less (~ 13%) than that exposed to PLLA ($n=8$, $p<0.05$).

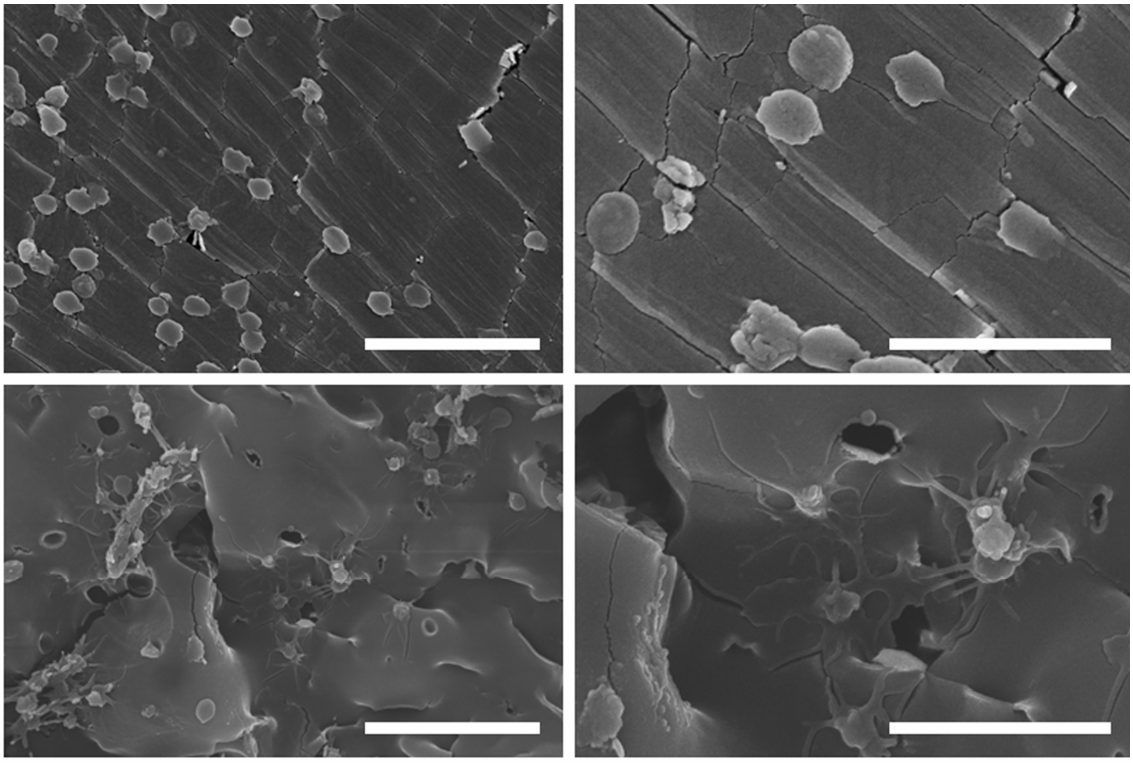

Fig 4.1 Evaluation of Platelet adhesion and aggregation using SEM. Platelets on CUPE (A, B) and PLLA (C, D) discs were observed at same magnification. A, C – 2000x, Scale bar = 20 μm; B, D – 5000x, Scale bar = 10 μm. Platelets on CUPE were spherical and those on PLLA were spread.

Thromboresistance is one of the primary design requirements for the construction of an ideal synthetic vascular graft [104-106]. The longer patency of thromboresistant grafts as compared to un-modified grafts further emphasizes the influence of thrombotic events on the lifetime of an artificial graft [9]. Although various modifications like immobilization of anti-thrombotic drugs and lumen endothelialization have been attempted to improve the thromboresistance of commonly available graft materials, it is more desirable to develop compliant materials which are inherently non thrombogenic. This will help circumvent long *in vitro* culture times and detachment of immobilized molecules, which are characteristic of endothelialization and immobilization techniques

respectively [107]. Results of platelet activation studies have indicated that CUPE adheres and activates lesser platelet numbers compared to PLLA, which implies that CUPE is less likely to initiate thrombosis when used as a vascular graft substitute *in vivo*.

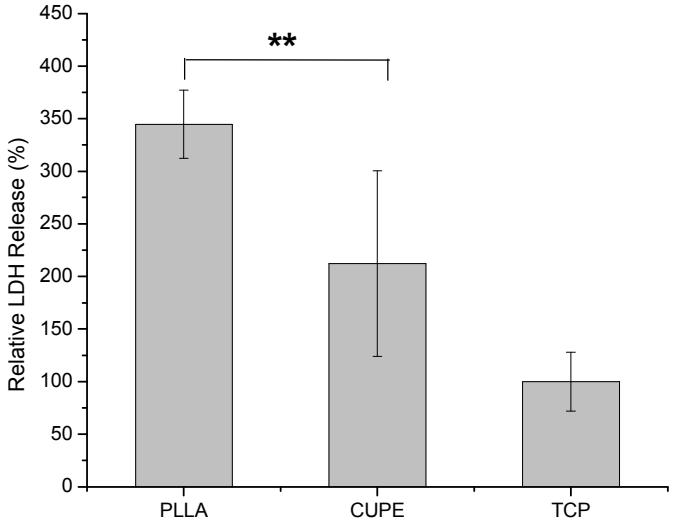


Fig 4.2 Quantification of platelet adhesion on the surface of PLLA, CUPE and TCP by lactate dehydrogenase assays. TCP served as control and all readings were normalized to LDH activity of TCP. The absorption at 490 nm relates linearly with adhered platelet numbers. ** corresponds to $p<0.01$, all groups have $N = 8$.

*4.3.3 Whole Blood Clotting Kinetics*

Formation of a blood clot or coagulation is a complicated process which involves the activation of a cascade of coagulation factors. The intrinsic pathway of coagulation is initiated by surface mediated reactions [108] and hence, determining the rate of clot formation after material contact enables us to evaluate the tendency of the material to promote thrombus formation. Evaluation of whole blood clotting kinetics also assumes

significance when it is taken into account that, coagulation, platelet activation and subsequent inflammation are interdependent processes. Higher absorbance values in this assay indicated that lesser number of red blood cells were involved in clot formation and

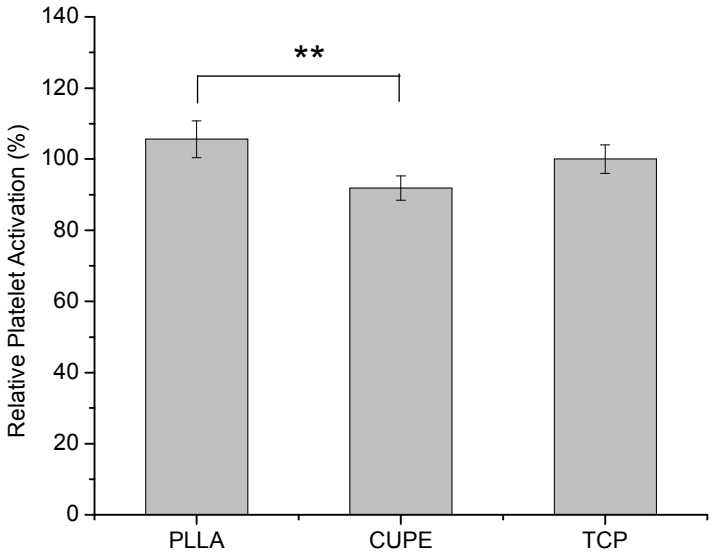


Fig 4.3 Determination of platelet activation by measuring the expression of membrane p-selectin on the platelet plasma membrane. p-selectin on platelets incubated with CUPE and PLLA samples (N=8), was tagged with fluorophore conjugated CD62p monoclonal antibodies. Readings were normalized with respect to p-selectin expression on platelets treated with TCP (control samples). * represents $p<0.05$ and ** corresponds to a p value $<0.01$. N = 8 in all groups.

therefore, corresponded to reduced coagulation. As shown in Figure 4.4, the absorbance measured from whole blood treated with PLLA, CUPE and TCP, kept decreasing till 60 minutes after material contact, indicating the formation of an incomplete thrombus.

On the other hand, complete thrombus formation took place within 30 minutes on glass. Compared to PLLA, no significant difference was found, in the clotting rate with respect to CUPE at each time point ($p>0.05$, n=8). This indicated that CUPE has similar

to or a little better thromboresistant properties than PLLA, which is a FDA approved material. The thromboresistant properties of CUPE may be attributed to uses of citric acid, which has been used as a commercial anticoagulant in the hospital, as one of the monomers in the polymer network.

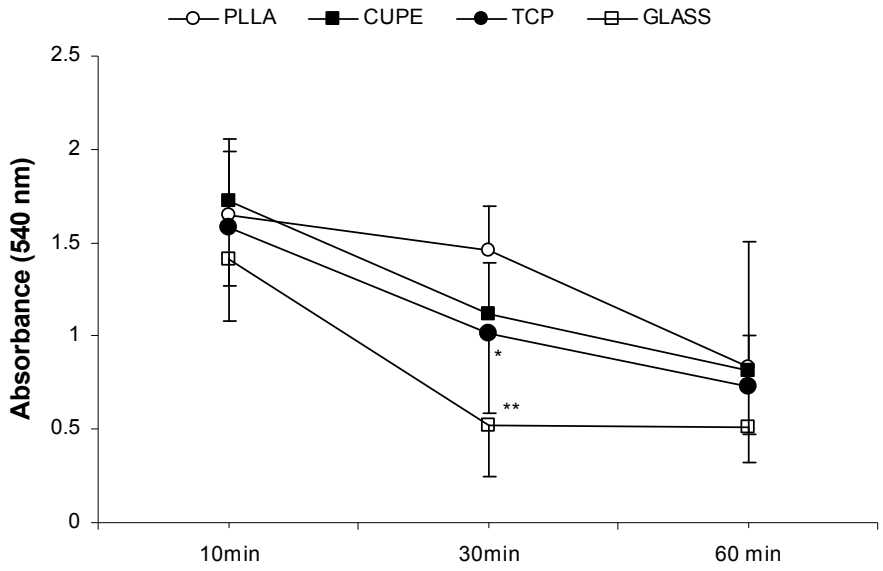


Fig 4.4 The effect of CUPE, PLLA, TCP and glass on initiating clotting in whole blood at different time points. Higher absorbance corresponds to greater number of free blood cells and hence lesser tendency of the material to initiate thrombus formation. * and ** correspond to $p<0.05$ and $p<0.01$ respectively, compared to PLLA

*4.3.4 Leukocyte Activation*

Implanted biomaterials elicit an acute inflammatory response, due to the irreversible adsorption of fibrinogen on the material surface; this leads to the attraction of and interaction with inflammatory cells on the implant [109]. Activated leukocytes show the up regulation of several distinct membrane protein receptors which allow them to

bind to platelets and endothelium during the inflammatory process [110]. CD11b macrophage-1 antigen (Mac-1) is a membrane glycoprotein expressed on activated leukocytes, including lymphocytes, monocytes, granulocytes, and a subset of natural killer (NK) cells. CD11b functions in cell-cell and cell substrate interactions, mediates inflammation by regulating leukocyte adhesion and migration, and has also been implicated in immune responses such as phagocytosis, cell-mediated cytotoxicity, chemotaxis and cellular activation [111]. The expression of CD11b/Mac-1 was used to determine the degree of leukocyte activation [112]. In our study, no significant difference in CD11b expression on leukocytes was found between CUPE and PLLA, suggesting that CUPE could have similar inflammation as FDA approved PLLA when implanted (Fig 4.5).

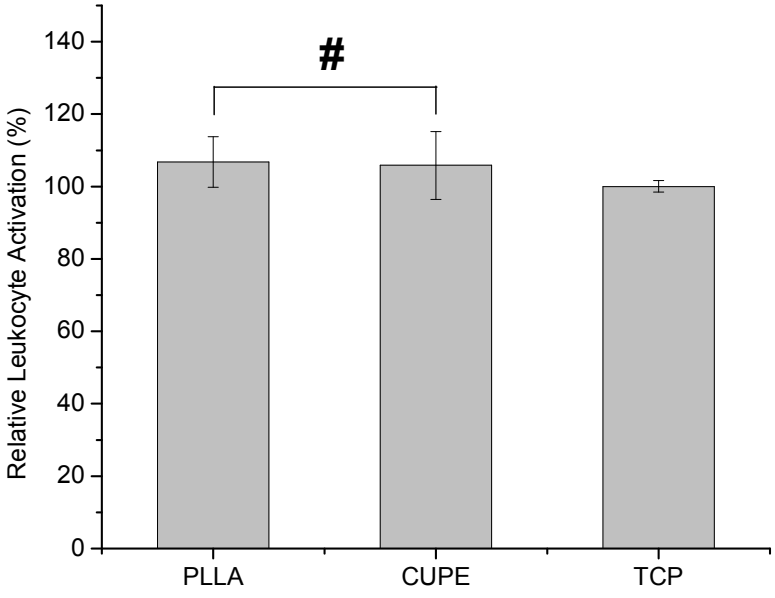


Fig 4.5 Assessment of leukocyte activation in whole blood by measuring MAC-1 antigen expression using flow cytometry. # corresponds to a $p > 0.05$. N = 8 for all groups.

*4.3.5 Cytokine (IL-1β and TNF-α) Release*

The inflammatory response generated by a biomaterial is also dependent on cytokines, which serve as signaling proteins. Cytokines are produced by a wide variety of hematopoietic and non-hematopoietic cell types. Tumor necrosis factor alpha (TNF-α) and interleukin 1 beta (IL-1β) are two of the best known pro-inflammatory cytokines. In the absence of exogenous stimuli, they are primarily released by activated monocytes and macrophages, at low concentrations in the blood. However, upon activation, there is an increase in the synthesis and release of these cytokines from the leukocytes. The higher cytokine concentration goes on to further influence the inflammatory process [113]. Both, TNF-α and IL-1β are associated with the up regulation of complimentary adhesion molecules on the vascular endothelium and leukocytes in the vicinity of vascular damage. Measured concentration of these cytokines has been extensively used previously as hemocompatibility markers [69, 90, 114]. In this study, CUPE exposed blood samples had significantly lower concentration of TNF-α (4.89±1.52 pg/ml, $p<0.05$, $n=7$) compared to PLLA treated blood samples (10.15±3.027 pg/ml) (Fig 4.6a). PLLA samples also released a higher concentration of IL-1β (11.58±1.86 pg/ml) compared to CUPE samples (5.48±2.16 pg/ml, $p<0.05$, $n=7$) (Fig 4.6b).

The degree of leukocyte activation combined with the release of cytokines provides an insight into the ability of the polymer surfaces to initiate an inflammatory response. Although flow cytometry analysis revealed similar degrees of leukocyte activation, the lower cytokine concentrations indicate that a less intense inflammatory response is elicited by CUPE compared to PLLA.

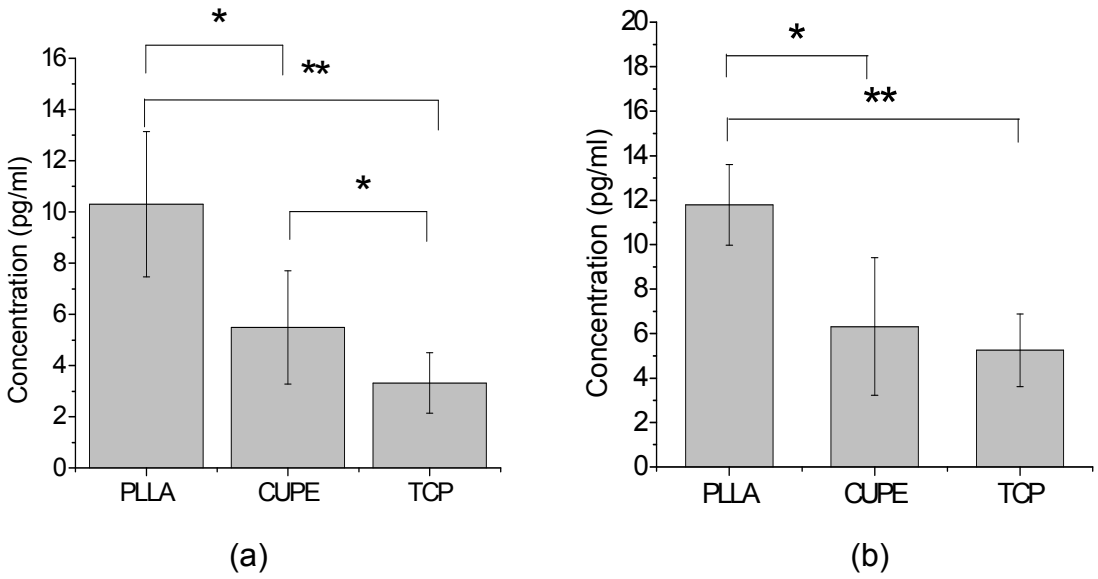


Fig 4.6 The amount of TNF-α (a) and IL-1β (b) released by leukocytes upon incubation of whole blood with PLLA, CUPE and TCP samples, as determined by flow cytometry. * corresponds to $p<0.05$ compared to PLLA and ** indicates a $p<0.01$ compared to PLLA.

*4.3.6 Hemolysis*

Hemolysis analysis was conducted to quantify the potential of CUPE to damage red blood cells. The concentration of which was released by damaged red blood cells was measured photospectrometrically and was correlated to material toxicity on the red blood cells [94]. As shown in Figure 4.7, biomaterial-mediated hemolysis was found to be <0.5% for both CUPE and PLLA, with no significant difference between them. Completely hemolysed blood in DI water was the positive control (PC). ** corresponds to a $p<0.01$ compared to positive control. N = 8 for all groups. Neither CUPE nor PLLA were observed to promote hemolysis. The results were similar to the previously reported POC that POC also does not promote hemolysis [69].

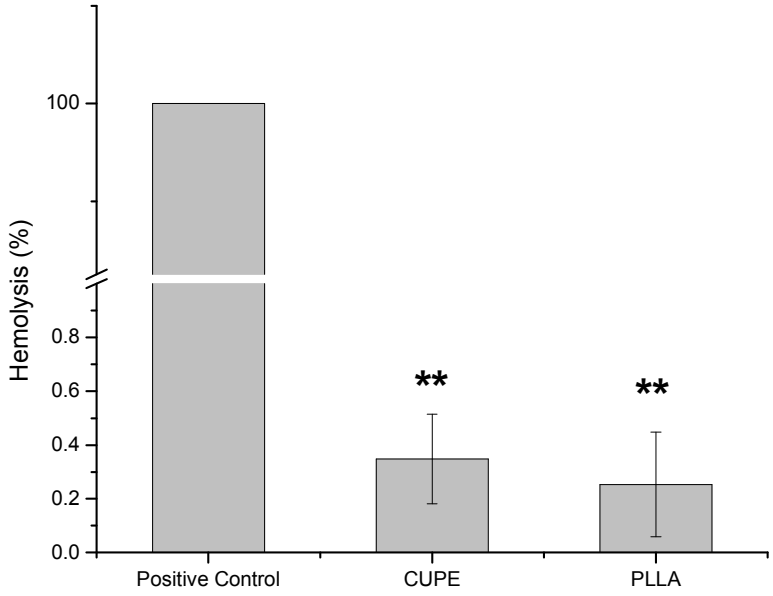


Fig 4.7 Percentage hemolysis of red blood cells after incubation of whole blood with PLLA and CUPE discs. Blood samples which did not contact any polymer served as negative control (NC) and completely hemolysed blood in DI water was the positive control (PC). ** corresponds to a $p<0.01$ compared to positive control. N = 8 for all groups.

## 4.4 Conclusion

In this study, the hemocompatibility of the new biodegradable elastic polymer, CUPE was evaluated *in vitro* by assessing the platelet adhesion and activation, blood clotting, leukocyte activation, inflammatory cytokine release and red blood cell hemolysis. The data collected showed that CUPE is less prone to thrombosis and inflammation, compared to PLLA. Neither does it trigger severe hemolysis. It could be concluded that doping urethane into polyester network did not compromise the hemocompatibility of polymers. Results from our studies implied this newly developed CUPE may be suitable for its intended use as vascular scaffold material and warrants further study in the vascular tissue engineering. Future studies include assessing the effect of CUPE on blood in a dynamic flow setting.

# CHAPTER 5

# CURRENT AND FUTURE WORK

One of the aspects of current work is focused on developing a family of CUPE polymers with different properties, by changing the pre-cursor used for the synthesis of CUPEs. In previous sections we have used POC as the representative pre-polymer for the synthesis of CUPEs. Work in progress includes synthesis and characterization of CUPEs with different properties, obtained by using different pre-cursor.

The biocompatibility and hemocompatibility studies indicate that CUPE scaffolds may act as suitable templates for vascular tissue engineering. In order to test this hypothesis, current work is also focused on the development of tubular scaffolds and bi-phasic tubular scaffolds.

## 5.1 Family of CUPE Polymers

### *5.1.1 Introduction*

It has been mentioned in the preceding sections that the careful choice of a diol is one of the three ways to modulate the properties of CUPE for designing application specific polymers. Whereas, the effect of isocyanate concentration and polymerization conditions on polymer properties have been examined in depth in earlier chapters, the effect of the choice of diol on polymer properties has received little attention. By changing the diol used, it is possible to produce new polymers with different mechanical,

degradation, thermal and bulk properties. The current work is focused on developing a family of crosslinked urethane doped polyesters, with varying properties which are obtained as a result of changing the diol used in the synthesis. The diols being used include a. 1,4-butane diol; b. 1,6-hexane diol; c. 1,10-decane diol; and d. 1,12-dodecane diol.

*5.1.2 Synthesis*

Like 1,8-octane diol, these pre-cursors are bulk polymerized with citric acid to form linear polyesters, which are further chain extended using HDI to obtain the different CUPEs. The different pre-cursors obtained include a. poly(1,4-butane diol) citrate (PBC); b. poly(1,6-hexane diol) citrate (PHC); c. poly(1,10-decane diol) citrate (PDC); and d. poly(1,12-dodecane diol) citrate (PDDC). Briefly, the diol was reacted with citric acid in a three neck reaction flask fitted with an inlet and outlet adapter. After the mixture had melted at 160 °C, the temperature was lowered to 140 °C. The reaction mixture was kept under stirring for further 60 minutes to create the pre-polymers. After purification these pre-cursor polymers were chain extended using HDI. Briefly, the purified pre-polymers were dissolved in dioxane to form a 3% solution (wt/wt). This solution was reacted with HDI in a clean and dry reaction flask under constant stirring, with stannous octoate as the catalyst at 55 °C. Reaction completion was monitored through periodic FT-IR measurements. A constant molar feed ratio of pre-polymer:HDI (1.2) was used for all the reactions.

This family of CUPEs obtained was abbreviated as CA-XY-U, where CA refers to the citric acid, XY refers to the diol used and U represents the urethane. The candidates for XY may be BD (butane diol), HD (hexane diol), DD (decane diol) and DDD (do-decane diol). Unless otherwise mentioned, the use of the term CUPE is applicable only for crosslinked urethane doped polyesters containing 1,8-octane diol as the diol portion.

### *5.1.3 Polymer Characterization*

#### 5.1.3.1 Infra-Red (IR) Measurements

FT-IR data was obtained as mentioned in previous sections. Briefly, a dilute solution of a 3% solution (wt/wt) of the different pre-CUPE polymers was cast on a clean KBr crystal. After all the solvent had evaporated, the spectra for each of the different pre-CUPEs were recorded. From the results obtained (Fig 5.1) it can be seen that in all cases, the reaction had completed, as denoted by the absence of the isocyanate peak at 2270 $cm^{-1}$. All the different pre-CUPE polymers demonstrate the presence of amide I and amide II peaks at 1670 $cm^{-1}$ and 1560 $cm^{-1}$ respectively. The height of the methylene peaks at 2931 $cm^{-1}$ increased with respect to the height of the carbonyl peaks at 1733 $cm^{-1}$ with increase in the number of methylene units in the diol used in the synthesis. CA-DDD-U had the highest methylene peaks in comparison to its carbonyl group, while CA-BD-U had the smallest. A broad urethane peak at 3350 $cm^{-1}$ was observed in each of the different pre-CUPEs tested.

5.1.3.2 Contact Angle Measurement

The initial contact angles of the different pre-CUPE polymers were measured as previously mentioned. From Fig 5.2 it can be observed that the contact angles of the pre-CUPE polymers increased with the use of diols which had larger number of methylene units. Pre-CA-DDD-U was the most hydrophobic (98.9106±1.344) while pre-CA-BD-U

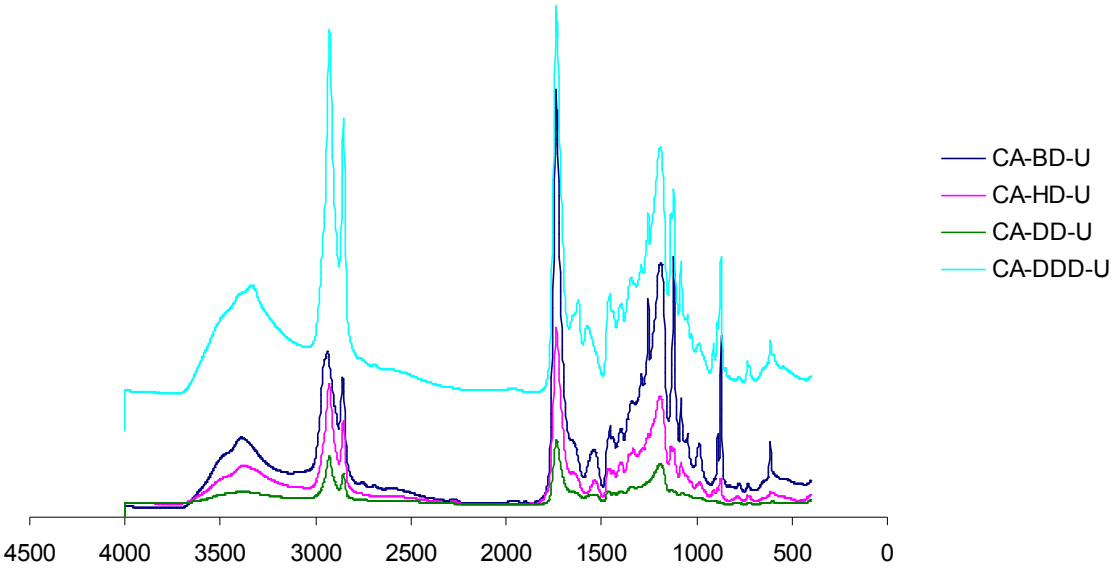


Fig 5.1 FT-IR spectra of the different pre-CUPE polymers.

was most hydrophilic (77.275±1.285) of all the different pre-CUPE polymers tested. This further corroborates the results obtained from the earlier study using different ratios of PEG in the polymer backbone. Changing the hydrophilicity of the diol segment, will result in changes in the surface properties of the different CUPEs as well.

5.1.3.3 Water Uptake Studies

Water uptake studies were conducted in phosphate buffer solution (PBS, pH 7.4) to determine if changing the diol monomer had any effect on the bulk properties of the CUPE family. Briefly, solutions of the different CUPE family members in dioxane (3% wt/wt) were cast into Teflon molds and allowed to dry in a chemical hood equipped with

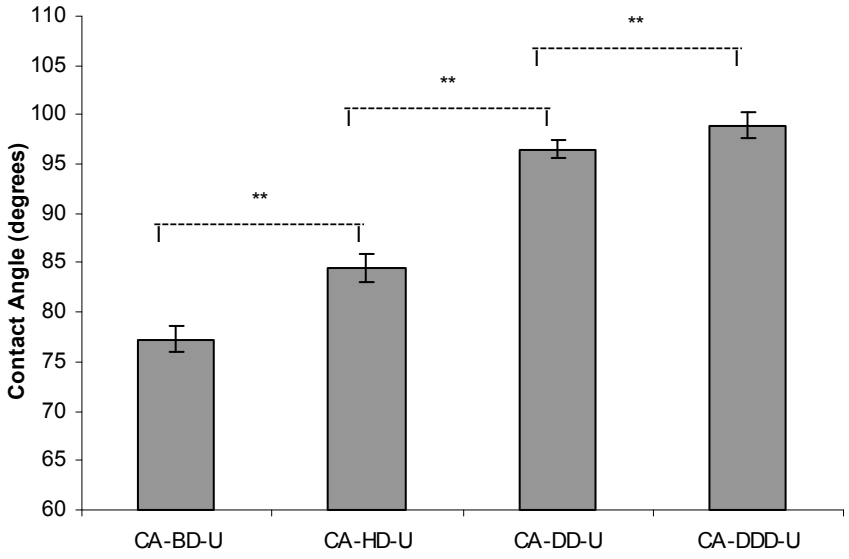


Fig 5.2 Initial contact angles of the different CUPE pre-polymers. Readings were taken for each specimen and averaged (N = 6). The hydrophobicity of the pre-polymers increased with increasing number of methylene units in the polymer chain. * corresponds to $p<0.05$, ** represents $p<0.01$.

a laminar air flow. Once all the solvent had evaporated, the molds were post-polymerized in a vacuum oven maintained at 80 °C for two days. The films were cut into disc shaped samples of diameter 10 mm and weighed to obtain the dry weight of the samples ($W_d$). 10 samples per CUPE polymer were used for the study. After noting the dry weight, the

samples were immersed in 10 ml of PBS kept at room temperature. At the end of 3 days, the samples were carefully removed from the PBS and dabbed lightly on both surfaces with a wipe to remove small water droplets, and weighed again to obtain the wet weight of the sample ($W_w$). The dry weight was then subtracted from the wet weight to determine the amount of PBS that was uptaken by the CUPE polymers. The results are presented in Fig 5.3. Once again, it can be observed that, with increasing number of methylene units in the diol monomer, the amount of water uptaken kept decreasing. CA-DDD-U had the lowest uptake (0.0038±0.001 g) while CA-BD-U had the highest uptake (0.0742±0.003 g). This can be attributed to the 12 methylene units in the 1,12-dodecane diol monomer compared to the 4 methylene units in the 1,4-butane diol monomer. Thus we can see that choosing a more hydrophilic diol for the synthesis of the CUPE polymer would result in a polymer with hydrophilic surface and bulk properties.

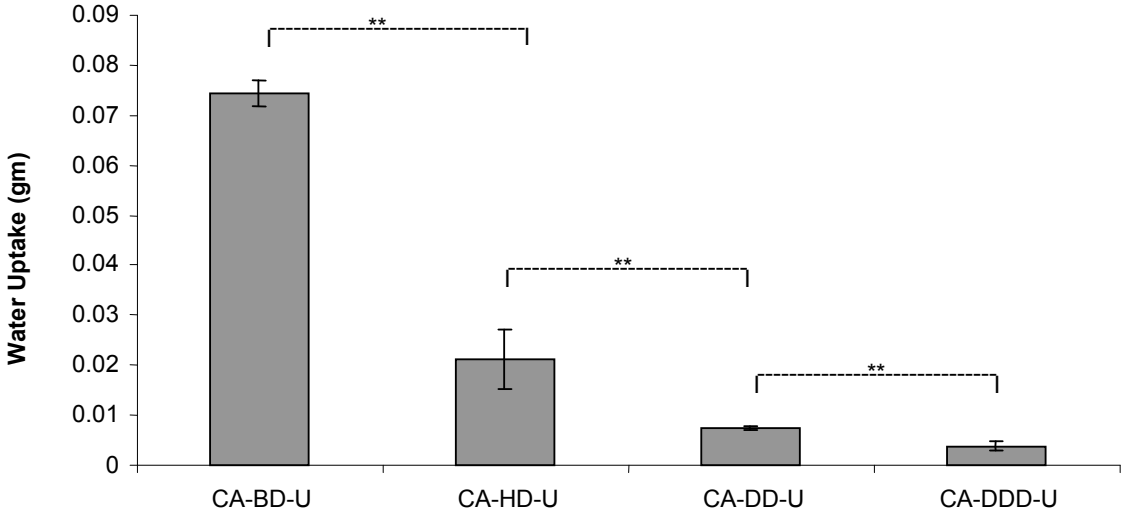


Fig 5.3 Water uptake of the different CUPE family members. Samples were post polymerized for 2 days at 80 °C prior to the study. ** represents $p<0.01$. N = 10.

5.1.3.4 In Vitro Degradation

In vitro degradation studies were performed in 0.01 M NaOH solutions. Films of the different family members were cut into discs of diameter 10 mm using a cork borer. After noting the initial weights of these polymer discs, they were immersed in test tubes containing 10 ml of NaOH. At pre-set time points, the samples were retrieved from the NaOH and washed three times in DI water to remove any trace NaOH. The sample weights were noted once again after lyophilization for 3 days. The mass loss of the sample was determined as per Equation 2.2. The degradation study data for CA-DDD-U has not been presented since it did not undergo any significant amount of degradation. From Fig 5.4 it can be seen that CA-BD-U had the fastest rate of degradation and was totally degraded within 9 hours. At 12 hours CA-HD-U was degraded to 26.3%±13.02% of its initial weight. In contrast, CA-DD-U had degraded by less than 5% with 96.68%±0.97% of its initial mass still intact. This trend can be attributed to the more hydrophilic surface and bulk of the CUPEs synthesized with the lower methylene unit containing monomers. The greater NaOH uptake would allow the NaOH to rapidly degrade the ester crosslinks and the ester bonds on the polymer backbone of CA-BD-U and CA-HD-U. On the other hand, the hydrophobic nature of CA-DD-U and CA-DDD-U would allow little amounts of NaOH to be uptaken and hence result in a slower rate of degradation.

5.1.3.5 In Vitro Cell Culture

Cells were seeded on the different CUPE family members to test their suitability as biomaterials. NIH 3T3 fibroblasts was chosen as the model cell line for this study.

Briefly, 7 mm discs were cut from the different CUPE films and sterilized by immersing in ethanol for 30 minutes, followed by 30 minutes of ultra-violet radiation (UV) treatment. The sterilized polymer discs were washed with excess PBS to remove traces of alcohol. Sterile discs were immersed in incomplete media for 12 hours prior to the

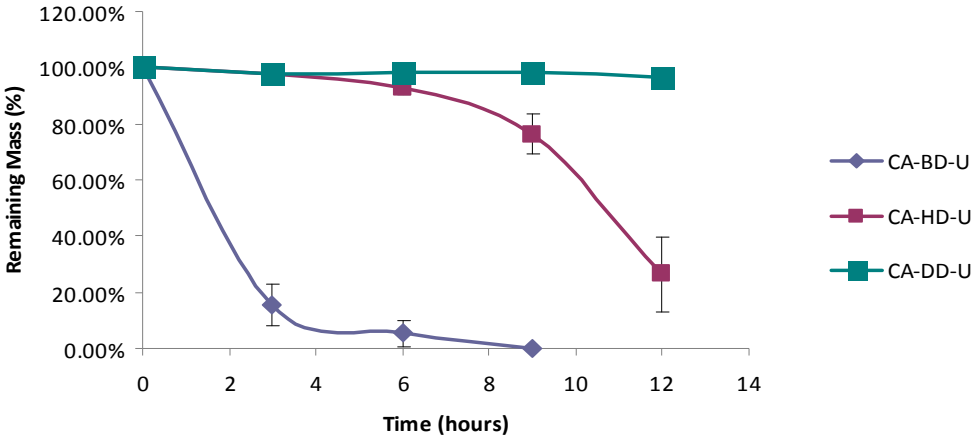


Fig 5.4 NaOh Degradation profiles of the different CUPE polymer family members. All the polymers used had been polymerized for 2 days at 80 °C.

seeding. A cell density of $3x10^5$ cells/ml was used for seeding. 200 µl of the cell suspension was distributed uniformly over the surface of the CUPE discs and allowed to incubate for 1 hour at 37 °C in an incubator. After this time, 5 ml of media was added to the culture dishes containing the disc samples. 3 days after seeding, the polymer discs were transferred to fresh culture plates and fixed by addition of 2.5% gluteraldehyde-PBS solution. Photomicrographs of the cells on the polymer surface were collected using a Leica DMLP microscope fitted with a Nikon E500 camera (Nikon Corp. Japan). From the images obtained (Fig 5.5), it was observed that the fibroblasts grew and proliferated over the surface of different CUPE polymers. The cells showed regular fibroblast

morphology and no surface treatments of the CUPE polymers were necessary to encourage cell growth. This provides some preliminary indication that the different polymer members of the CUPE family are not adverse to cellular growth.

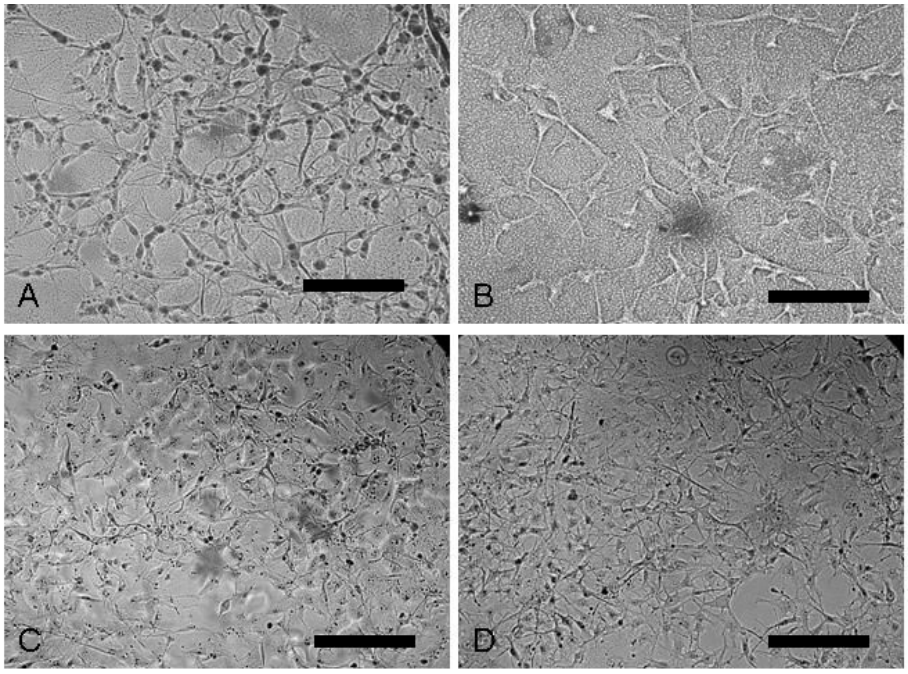


Fig 5.5 Photomicrographs of 3T3 fibroblasts which have proliferated over the surface of the different CUPE polymers. a. CA-BD-U; b. CA-HD-U; c. CA-DD-U; d. CA-DDD-U. Scale bars correspond to 100 μm.

## 5.2 Bi-Phasic Scaffold Design

### *5.2.1 Introduction*

A tubular bi-phasic scaffold was fabricated to demonstrate the potential of CUPE to function as a vascular graft template. The concept of a bi-phasic scaffold was first realized by Yang et al and is an attempt to mimic the architecture of a native vessel. The bi-phasic scaffold comprises of a non porous inner lumen with a porous outer layer. Endothelial cells (ECs) may be seeded in the lumen and smooth muscle cells may be

seeded in the porous outer layer (SMCs). The non porous nature of the lumen would serve to isolate the ECs from the SMCs.

*5.2.2 Fabrication and Preliminary Characterization*

The bi-phasic scaffold was fabricated in two steps.

In step 1, a glass rod was dipped in a solution of CUPE in dioxane (5% wt/wt). The glass rod was suspended till the polymer formed a smooth layer on the glass rod and all the solvent had evaporated. The coating process was repeated till a uniform CUPE film was obtained on the glass rod.

In step 2, CUPE solution (5% wt/wt) in dioxane was mixed with salt in a 1:9 ratio of polymer to salt. This mixture was kept under constant stirring till most of the solvent had evaporated and a thick slurry was obtained. In order to form the porous outer layer, the film coated glass rod was rolled in this slurry till an even layer of polymer-salt was formed on the glass rod.

The glass rod was post polymerized in an 80 °C oven for 2 days. During post polymerization, ester bonds were formed between the CUPE film on the inner layer and the CUPE polymer in the porous outer layer, binding them together co-valently. After curing, this construct was placed in excess water in order to get rid of all the salt. The water was replaced every 12 hours till all the salt had dissolved.

SEM analysis of the cross-section revealed the biphasic nature of the scaffold (Fig 5.6). The non porous inner lumen formed a continuous layer without any breaks. The cross-section of the porous layer showed good inter-connectivity with a few dead pores.

Further experiments for characterizing these bi-phasic scaffolds, including seeding them with ECs and SMCs is currently in progress.

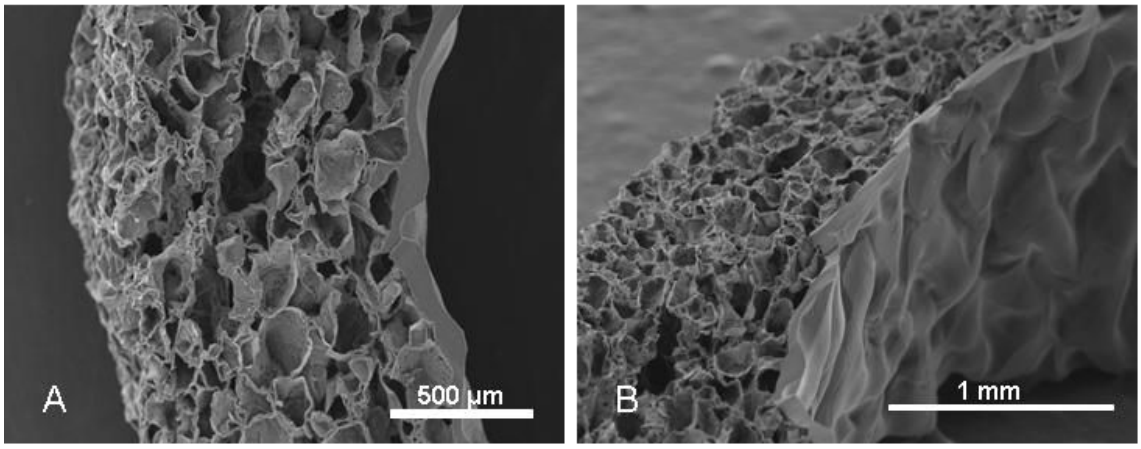


Fig 5.6 Cross sectional SEM images of a bi-phasic tubular CUPE scaffold. A. Pore sizes for porous layer were in the range of 150-200 µm. Both dead pores and inter-connected pores may be observed. B. CUPE film formed a continuous non porous lumen with no breaks or cracks.

# CHAPTER 6

# CONCLUSION

The overall goal of our project was to develop a soft, elastic and strong material for vascular tissue engineering. The specific aims were to synthesize and characterize this material, ensuring that it had improved mechanical properties compared to existing crosslinked polyesters, like POC and to evaluate its biocompatibility and in particular its hemocompatibility. We successfully synthesized and characterized this new family of polymers, crosslinked urethane doped polyesters (CUPEs) and demonstrated that it had properties which were well suited for vascular tissue engineering. CUPEs were synthesized by doping the polyester network of POC with urethane linkages. XRD and thermal property analysis indicated that the materials were totally amorphous. The tensile strength of CUPE was as high as 41.07±6.85 MPa with corresponding break strains of 222.66±27.84%. This is a significant improvement upon the mechanical properties of POC (2.93±0.09 MPa). The Young's Modulus ranged from 4.14±1.71 MPa to 38.35±4.5 MPa indicating that by varying the different synthesis parameters we could produce CUPEs which ranged from being soft materials to tough and rigid materials. The degradation rate of CUPE could also be controlled by varying the choice of monomeric diol used, the polymerization conditions and the concentration of urethane linkages in the polymer network. The polymers supported growth and proliferation of NIH 3T3 fibroblasts and human aortic smooth muscle cells. MTT assay and in vivo implantation

indicate that the biocompatibility performance of CUPE is comparable, if not better than PLLA. In addition to being biocompatible, hemocompatibility evaluation revealed that CUPE adhered and activated lesser number of platelets compared to PLLA, indicating that CUPE may be less thrombogenic. Inflammatory potential of CUPE was comparable to PLLA. CUPE also did not contribute to any hemolysis. CUPE was used to fabricate bi-phasic scaffolds which had a continuous inner lumen and a porous outer shell.

This study has resulted in the availability of a new polymer which has improved properties over both crosslinked polyester networks and biodegradable polyurethanes. These materials were stronger than crosslinked polyesters and preserved their good biocompatibility. Additionally, these materials were able to regain their original dimensions unlike polyurethanes which underwent permanent deformation. Following these results it is expected that CUPE may be able to design scaffolds which meet the requirements of an ideal small diameter vascular grafts.

REFERENCES

1. Moreno JJ, Mitjavila MT. The degree of unsaturation of dietary fatty acids and the development of atherosclerosis (review). J Nutr Biochem 2003 Apr;14(4):182-195.

2. Ratcliffe A. Tissue engineering of vascular grafts. Matrix Biol 2000 Aug;19(4):353-357.

3. Conte MS. The ideal small arterial substitute: a search for the Holy Grail? FASEB J 1998 Jan;12(1):43-45.

4. Mitchell SL, Niklason LE. Requirements for growing tissue-engineered vascular grafts. Cardiovasc Pathol 2003 Mar-Apr;12(2):59-64.

5. L'Heureux N, Dusserre N, Marini A, Garrido S, de la Fuente L, McAllister T. Technology insight: the evolution of tissue-engineered vascular grafts--from research to clinical practice. Nat Clin Pract Cardiovasc Med 2007 Jul;4(7):389-395.

6. Wang X, Lin P, Yao Q, Chen C. Development of small-diameter vascular grafts. World J Surg 2007 Apr;31(4):682-689.

7. Pasic M, Muller-Glauser W, von Segesser L, Odermatt B, Lachat M, Turina M. Endothelial cell seeding improves patency of synthetic vascular grafts: manual versus automatized method. Eur J Cardiothorac Surg 1996;10(5):372-379.

8. Yang J, Motlagh D, Allen JB, Webb AR, Kibbe MR, Aalami O, et al. Modulating EPTFE vascular graft host response via citric acid based degradable polymers. Advanced Materials 2006;18(12):1493-1498.

9. Begovac PC, Thomson RC, Fisher JL, Hughson A, Gallhagen A. Improvements in GORE-TEX vascular graft performance by Carmeda BioActive surface heparin immobilization. Eur J Vasc Endovasc Surg 2003 May;25(5):432-437.

10. Faries PL, Logerfo FW, Arora S, Hook S, Pulling MC, Akbari CM, et al. A comparative study of alternative conduits for lower extremity revascularization: all-autogenous conduit versus prosthetic grafts. J Vasc Surg 2000 Dec;32(6):1080-1090.

11. Xue L, Greisler HP. Biomaterials in the development and future of vascular grafts. J Vasc Surg 2003 Feb;37(2):472-480.

12. Isenberg BC, Williams C, Tranquillo RT. Small-diameter artificial arteries engineered in vitro. Circ Res 2006 Jan 6;98(1):25-35.

13. Nerem RM, Seliktar D. Vascular tissue engineering. Annu Rev Biomed Eng 2001;3:225-243.

14. Bujan J, Garcia-Honduvilla N, Bellon JM. Engineering conduits to resemble natural vascular tissue. Biotechnol Appl Biochem 2004 Feb;39(Pt 1):17-27.

15. Teebken OE, Haverich A. Tissue engineering of small diameter vascular grafts. Eur J Vasc Endovasc Surg 2002 Jun;23(6):475-485.

16. Lee MC, Haut RC. Strain rate effects on tensile failure properties of the common carotid artery and jugular veins of ferrets. Journal of Biomechanics 1992;25(8):925-927.
17. Yang J, Motlagh D, Webb AR, Ameer GA. Novel biphasic elastomeric scaffold for small-diameter blood vessel tissue engineering. Tissue Eng 2005 Nov-Dec;11(11-12):1876-1886.

18. Tiwari A, Cheng KS, Salacinski H, Hamilton G, Seifalian AM. Improving the patency of vascular bypass grafts: the role of suture materials and surgical techniques on reducing anastomotic compliance mismatch. Eur J Vasc Endovasc Surg 2003 Apr;25(4):287-295.

19. Lemson MS, Tordoir JH, Daemen MJ, Kitslaar PJ. Intimal hyperplasia in vascular grafts. Eur J Vasc Endovasc Surg 2000 Apr;19(4):336-350.

20. Noordenbos J, Dore C, Hansbrough JF. Safety and efficacy of TransCyte for the treatment of partial-thickness burns. J Burn Care Rehabil 1999 Jul-Aug;20(4):275-281.

21. Naughton G, Mansbridge J, Gentzkow G. A metabolically active human dermal replacement for the treatment of diabetic foot ulcers. Artif Organs 1997 Nov;21(11):1203-1210.

22. Schreiber RE, Ilten-Kirby BM, Dunkelman NS, Symons KT, Rekettye LM, Willoughby J, et al. Repair of osteochondral defects with allogeneic tissue engineered cartilage implants. Clinical orthopaedics and related research 1999;367:382-395.

23. Baguneid MS, Seifalian AM, Salacinski HJ, Murray D, Hamilton G, Walker MG. Tissue engineering of blood vessels. Br J Surg 2006 Mar;93(3):282-290.
24. Stegemann JP, Kaszuba SN, Rowe SL. Review: advances in vascular tissue engineering using protein-based biomaterials. Tissue Eng 2007 Nov;13(11):2601-2613.

25. Weinberg CB, Bell E. A blood vessel model constructed from collagen and cultured vascular cells. Science 1986 Jan 24;231(4736):397-400.

26. L'Heureux N, Germain L, Labbe R, Auger FA. In vitro construction of a human blood vessel from cultured vascular cells: a morphologic study. J Vasc Surg 1993 Mar;17(3):499-509.

27. Miwa H, Matsuda T, Iida F. Development of a hierarchically structured hybrid vascular graft biomimicking natural arteries. ASAIO J 1993 Jul-Sep;39(3):M273-277.
28. Seliktar D, Black RA, Vito RP, Nerem RM. Dynamic mechanical conditioning of collagen-gel blood vessel constructs induces remodeling in vitro. Ann Biomed Eng 2000 Apr;28(4):351-362.

29. Kanda K, Matsuda T. Mechanical stress-induced orientation and ultrastructural change of smooth muscle cells cultured in three-dimensional collagen lattices. Cell Transplant 1994 Nov-Dec;3(6):481-492.

30. Hong H, McCullough CM, Stegemann JP. The role of ERK signaling in protein hydrogel remodeling by vascular smooth muscle cells. Biomaterials 2007 Sep;28(26):3824-3833.

31. Ogle BM, Mooradian DL. The role of vascular smooth muscle cell integrins in the compaction and mechanical strengthening of a tissue-engineered blood vessel. Tissue Eng 1999 Aug;5(4):387-402.

32. Swartz DD, Russell JA, Andreadis ST. Engineering of fibrin-based functional and implantable small-diameter blood vessels. Am J Physiol Heart Circ Physiol 2005 Mar;288(3):H1451-1460.

33. Berglund JD, Mohseni MM, Nerem RM, Sambanis A. A biological hybrid model for collagen-based tissue engineered vascular constructs. Biomaterials 2003 Mar;24(7):1241-1254.

34. Wissink MJ, van Luyn MJ, Beernink R, Dijk F, Poot AA, Engbers GH, et al. Endothelial cell seeding on crosslinked collagen: effects of crosslinking on endothelial cell proliferation and functional parameters. Thromb Haemost 2000 Aug;84(2):325-331.
35. Gratzer PF, Pereira CA, Lee JM. Solvent environment modulates effects of glutaraldehyde crosslinking on tissue-derived biomaterials. J Biomed Mater Res 1996 Aug;31(4):533-543.

36. Girton TS, Oegema TR, Grassl ED, Isenberg BC, Tranquillo RT. Mechanisms of stiffening and strengthening in media-equivalents fabricated using glycation. J Biomech Eng 2000 Jun;122(3):216-223.

37. Berglund JD, Nerem RM, Sambanis A. Incorporation of intact elastin scaffolds in tissue-engineered collagen-based vascular grafts. Tissue Eng 2004 Sep-Oct;10(9-10):1526-1535.

38. Buttafoco L, Kolkman NG, Engbers-Buijtenhuijs P, Poot AA, Dijkstra PJ, Vermes I, et al. Electrospinning of collagen and elastin for tissue engineering applications. Biomaterials 2006 Feb;27(5):724-734.

39. Boland ED, Matthews JA, Pawlowski KJ, Simpson DG, Wnek GE, Bowlin GL. Electrospinning collagen and elastin: preliminary vascular tissue engineering. Front Biosci 2004 May 1;9:1422-1432.

40. Grassl ED, Oegema TR, Tranquillo RT. Fibrin as an alternative biopolymer to type-I collagen for the fabrication of a media equivalent. J Biomed Mater Res 2002 Jun 15;60(4):607-612.

41. Cummings CL, Gawlitta D, Nerem RM, Stegemann JP. Properties of engineered vascular constructs made from collagen, fibrin, and collagen-fibrin mixtures. Biomaterials 2004 Aug;25(17):3699-3706.

42. Schaner PJ, Martin ND, Tulenko TN, Shapiro IM, Tarola NA, Leichter RF, et al. Decellularized vein as a potential scaffold for vascular tissue engineering. J Vasc Surg 2004 Jul;40(1):146-153.

43. Amiel GE, Komura M, Shapira O, Yoo JJ, Yazdani S, Berry J, et al. Engineering of blood vessels from acellular collagen matrices coated with human endothelial cells. Tissue Eng 2006 Aug;12(8):2355-2365.

44. Huynh T, Abraham G, Murray J, Brockbank K, Hagen PO, Sullivan S. Remodeling of an acellular collagen graft into a physiologically responsive neovessel. Nat Biotechnol 1999 Nov;17(11):1083-1086.

45. Kaushal S, Amiel GE, Guleserian KJ, Shapira OM, Perry T, Sutherland FW, et al. Functional small-diameter neovessels created using endothelial progenitor cells expanded ex vivo. Nat Med 2001 Sep;7(9):1035-1040.

46. Hilbert SL, Ferrans VJ, Jones M. Tissue derived biomaterial and their use in cardiovascular prosthetic devices. Medical Progress through Technology 1989;14:115-163.

47. Schmidt CE, Baier JM. Acellular vascular tissues: natural biomaterials for tissue repair and tissue engineering. Biomaterials 2000 Nov;21(22):2215-2231.

48. Lu Q, Ganesan K, Simionescu DT, Vyavahare NR. Novel porous aortic elastin and collagen scaffolds for tissue engineering. Biomaterials 2004 Oct;25(22):5227-5237.

49. Eybl E, Griesmacher A, Grimm M, Wolner E. Toxic effects of aldehydes released from fixed pericardium on bovine aortic endothelial cells. Journal of Biomedical Materials Research 1989;23:1355-1365.

50. Stitzel JD, Pawlowski KJ, Wnek GE, Simpson DG, Bowlin GL. Arterial smooth muscle cell proliferation on a novel biomimicking, biodegradable vascular graft scaffold. J Biomater Appl 2001 Jul;16(1):22-33.

51. Schmidt D, Breymann C, Weber A, Guenter CI, Neuenschwander S, Zund G, et al. Umbilical cord blood derived endothelial progenitor cells for tissue engineering of vascular grafts. Ann Thorac Surg 2004 Dec;78(6):2094-2098.

52. Niklason LE, Gao J, Abbott WM, Hirschi KK, Houser S, Marini R, et al. Functional arteries grown in vitro. Science 1999 Apr 16;284(5413):489-493.

53. Greisler HP. Arterial regeneration over absorbable prostheses. Arch Surg 1982 Nov;117(11):1425-1431.

54. Kannan RY, Salacinski HJ, Butler PE, Hamilton G, Seifalian AM. Current status of prosthetic bypass grafts: a review. J Biomed Mater Res B Appl Biomater 2005 Jul;74(1):570-581.

55. Shum-Tim D, Stock U, Hrkach J, Shinoka T, Lien J, Moses MA, et al. Tissue engineering of autologous aorta using a new biodegradable polymer The Annals of Thoracic Surgery 1999;68:2298.

56. Izhar U, Schwalb H, Borman JB, Hellener GR, Hotoveli-Salomon A, Marom G, et al. Novel synthetic selectively degradable vascular prostheses: a preliminary implantation study. J Surg Res 2001 Feb;95(2):152-160.

57. Greisler HP, Ellinger J, Schwarcz TH, Golan J, Raymond RM, Kim DU. Arterial regeneration over polydioxanone prostheses in the rabbit. Arch Surg 1987 Jun;122(6):715-721.

58. Kreklau B, Sittinger M, Mensing MB, Voigt C, Berger G, Burmester GR, et al. Tissue engineering of biphasic joint cartilage transplants. Biomaterials 1999 Sep;20(18):1743-1749.

59. Rohner D, Hutmacher DW, Cheng TK, Oberholzer M, Hammer B. In vivo efficacy of bone-marrow-coated polycaprolactone scaffolds for the reconstruction of orbital defects in the pig. J Biomed Mater Res B Appl Biomater 2003 Aug 15;66(2):574-580.

60. Lukashev ME, Werb Z. ECM signalling: orchestrating cell behaviour and misbehaviour. Trends Cell Biol 1998 Nov;8(11):437-441.

61. Stegemann JP, Hong H, Nerem RM. Mechanical, biochemical, and extracellular matrix effects on vascular smooth muscle cell phenotype. J Appl Physiol 2005 Jun;98(6):2321-2327.

62. Ingber DE. Cellular mechanotransduction: putting all the pieces together again. FASEB J 2006 May;20(7):811-827.

63. Wang Y, Ameer GA, Sheppard BJ, Langer R. A tough biodegradable elastomer. Nat Biotechnol 2002 Jun;20(6):602-606.

64. Yang J, Webb AR, Pickerill SJ, Hageman G, Ameer GA. Synthesis and evaluation of poly(diol citrate) biodegradable elastomers. Biomaterials 2006 Mar;27(9):1889-1898.

65. Guan J, Sacks MS, Beckman EJ, Wagner WR. Synthesis, characterization, and cytocompatibility of elastomeric, biodegradable poly(ester-urethane)ureas based on poly(caprolactone) and putrescine. J Biomed Mater Res 2002 Sep 5;61(3):493-503.

66. Guan J, Sacks MS, Beckman EJ, Wagner WR. Biodegradable poly(ether ester urethane)urea elastomers based on poly(ether ester) triblock copolymers and putrescine: synthesis, characterization and cytocompatibility. Biomaterials 2004 Jan;25(1):85-96.

67. Guan J, Wagner WR. Synthesis, characterization and cytocompatibility of polyurethaneurea elastomers with designed elastase sensitivity. Biomacromolecules 2005 Sep-Oct;6(5):2833-2842.

68. Yang J, Webb AR, Ameer GA. Novel Citric Acid-Based Biodegradable Elastomers for Tissue Engineering. Advanced Materials 2004;16:511-516.

69. Motlagh D, Allen J, Hoshi R, Yang J, Lui K, Ameer G. Hemocompatibility evaluation of poly(diol citrate) in vitro for vascular tissue engineering. J Biomed Mater Res A 2007 Sep 15;82(4):907-916.

70. Boretos JW, Pierce WS. Segmented polyurethane: a new elastomer for biomedical applications. Science 1967 Dec 15;158(807):1481-1482.

71. Wilson GJ, MacGregor DC, Klement P, Dereume JP, Weber BA, Binnington AG, et al. The composite Corethane/Dacron vascular prosthesis. Canine in vivo evaluation of 4 mm diameter grafts with 1 year follow-up. Asaio Transactions 1991;3:M475-M476.

72. Seifalian AM, Salacinski HJ, Tiwari A, Edwards A, Bowald S, Hamilton G. In vivo biostability of a poly(carbonate-urea)urethane graft. Biomaterials 2003 Jun;24(14):2549-2557.

73. Abraham GA, Marcos-Fernandez A, Roman JS. Bioresorbable poly(ester-ether urethane)s from L-lysine diisocyanate and triblock copolymers with different hydrophilic character. J Biomed Mater Res A 2006 Mar 15;76(4):729-736.

74. Yamamoto N, Nakayama A, Oshima M, Kawasaki N, Aiba S. Enzymatic hydrolysis of lysine diisocyanate based polyurethanes and segmented polyurethane ureas by various proteases. Reactive and Functional Polymers 2007;67:1338-1345.

75. Guelcher SA. Biodegradable polyurethanes: synthesis and applications in regenerative medicine. Tissue Eng Part B Rev 2008 Mar;14(1):3-17.

76. Guan J, Fujimoto KL, Sacks MS, Wagner WR. Preparation and characterization of highly porous, biodegradable polyurethane scaffolds for soft tissue applications. Biomaterials 2005 Jun;26(18):3961-3971.

77. Nieponice A, Soletti L, Guan J, Deasy BM, Huard J, Wagner WR, et al. Development of a tissue-engineered vascular graft combining a biodegradable scaffold, muscle-derived stem cells and a rotational vacuum seeding technique. Biomaterials 2008 Mar;29(7):825-833.

78. Spaans CJ, Groot JH, Dekens FG, Pennings AJ. High molecular weight polyurethanes and a polyurethane urea based on 1,4-butanediisocyanate. Polymer Bulletin 1998;41:131-138.

79. Skarja GA, Woodhouse KA. Synthesis and Characterization of degadable polyurethane elastomers containing an amino acid-based chain extender. Journal of Biomaterial Science, Polymer Edition 1998;9(3):271-295.

80. Kylma J, Seppala JV. Synthesis and characterization of a biodegradable thermoplastic poly(ester-urethane) elastomer. Macromolecules 1997;30:2877-2882.

81. Tatai L, Moore TG, Adhikari R, Malherbe F, Jayasekara R, Griffiths I, et al. Thermoplastic biodegradable polyurethanes: the effect of chain extender structure on properties and in-vitro degradation. Biomaterials 2007 Dec;28(36):5407-5417.

82. Lee CR, Grad S, Gorna K, Gogolewski S, Goessl A, Alini M. Fibrin-polyurethane composites for articular cartilage tissue engineering: a preliminary analysis. Tissue Eng 2005 Sep-Oct;11(9-10):1562-1573.

83. Skarja GA, Woodhouse KA. In vitro degradation and erosion of degradable, segmented polyurethanes containing an amino acid-based chain extender. J Biomater Sci Polym Ed 2001;12(8):851-873.

84. Yang J, Webb AR, Ameer GA. Novel Citric Acid-Based Biodegradable Elastomers for Tissue Engineering. Advanced Materials 2004;16(6):511-516.

85. Jayakumar R, Lee YS, Nanjundan S. Synthesis and characterization of calcium containing polyurethane ureas. Journal of Applied Polymer Science 2003;90(13):3488-3496.

86. Gorbet MB, Sefton MV. Biomaterial-associated thrombosis: roles of coagulation factors, complement, platelets and leukocytes. Biomaterials 2004 Nov;25(26):5681-5703.

87. Wendel HP, Ziemer G. Coating-techniques to improve the hemocompatibility of artificial devices used for extracorporeal circulation. Eur J Cardiothorac Surg 1999 Sep;16(3):342-350.

88. Llanos GR, Sefton MV. Immobilization of poly(ethylene glycol) onto a poly(vinyl alcohol) hydrogel: 2. Evaluation of thrombogenicity. J Biomed Mater Res 1993 Nov;27(11):1383-1391.

89. Hanson SR, Harker LA, Bjornsson TD. Effects of platelet-modifying drugs on arterial thromboembolism in baboons. Aspirin potentiates the antithrombotic actions of dipyridamole and sulfinpyrazone by mechanism(s) independent of platelet cyclooxygenase inhibition. J Clin Invest 1985 May;75(5):1591-1599.

90. Motlagh D, Yang J, Lui KY, Webb AR, Ameer GA. Hemocompatibility evaluation of poly(glycerol-sebacate) in vitro for vascular tissue engineering. Biomaterials 2006 Aug;27(24):4315-4324.

91. Berman CL, Yeo EL, Wencel-Drake JD, Furie BC, Ginsberg MH, Furie B. A platelet alpha granule membrane protein that is associated with the plasma membrane after activation. Characterization and subcellular localization of platelet activation-dependent granule-external membrane protein. J Clin Invest 1986 Jul;78(1):130-137.

92. Imai Y, Nose Y. A new method for evalution of antithrombogenicity of materials. J Biomed Mater Res 1972 May;6(3):165-172.

93. Huang N, Yang P, Leng YX, Chen JY, Sun H, Wang J, et al. Hemocompatibility of titanium oxide films. Biomaterials 2003 Jun;24(13):2177-2187.

94. Fischer D, Li Y, Ahlemeyer B, Krieglstein J, Kissel T. In vitro cytotoxicity testing of polycations: influence of polymer structure on cell viability and hemolysis. Biomaterials 2003 Mar;24(7):1121-1131.

95. Kuchulakanti PK, Chu WW, Torguson R, Ohlmann P, Rha SW, Clavijo LC, et al. Correlates and long-term outcomes of angiographically proven stent thrombosis with sirolimus- and paclitaxel-eluting stents. Circulation 2006 Feb 28;113(8):1108-1113.

96. Allen RD, Zacharski LR, Widirstky ST, Rosenstein R, Zaitlin LM, Burgess DR. Transformation and motility of human platelets: details of the shape change and release reaction observed by optical and electron microscopy. J Cell Biol 1979 Oct;83(1):126-142.

97. Tamada Y, Kulik EA, Ikada Y. Simple method for platelet counting. Biomaterials 1995 Feb;16(3):259-261.

98. Grunkemeier JM, Tsai WB, Horbett TA. Hemocompatibility of treated polystyrene substrates: contact activation, platelet adhesion, and procoagulant activity of adherent platelets. J Biomed Mater Res 1998 Sep 15;41(4):657-670.

99. Lin W-C, Tseng C-H, Yang M-C. In-Vitro Hemocompatibility Evaluation of a Thermoplastic Polyurethane Membrane with Surface-Immobilized Water-Soluble Chitosan and Heparin. Macromolecular Bioscience 2005;5:1013-1021.

100. Cholakis CH, Zingg W, Sefton MV. Effect of heparin-PVA hydrogel on platelets in a chronic canine arterio-venous shunt. J Biomed Mater Res 1989 Apr;23(4):417-441.

101. Gemmell CH, Ramirez SM, Yeo EL, Sefton MV. Platelet activation in whole blood by artificial surfaces: identification of platelet-derived microparticles and activated platelet binding to leukocytes as material-induced activation events. J Lab Clin Med 1995 Feb;125(2):276-287.

102. Murakami T, Komiyama Y, Masuda M, Kido H, Nomura S, Fukuhara S, et al. Flow cytometric analysis of platelet activation markers CD62P and CD63 in patients with coronary artery disease. Eur J Clin Invest 1996 Nov;26(11):996-1003.

103. Michelson AD. Flow cytometry: a clinical test of platelet function. Blood 1996 Jun 15;87(12):4925-4936.

104. Isenberg BC, Williams C, Tranquillo RT. Small-diameter artificial arteries engineered in vitro. Circulation Research 2006 JAN 6;98(1):25-35.

105. Tranquillo RT. The tissue-engineered small-diameter artery. Ann N Y Acad Sci 2002 Jun;961:251-254.

106. Ratcliffe A. Tissue engineering of vascular grafts. Matrix Biology 2000;19:353-357.

107. Hoenig MR, Campbell GR, Rolfe BE, Campbell JH. Tissue-engineered blood vessels: alternative to autologous grafts? Arterioscler Thromb Vasc Biol 2005 Jun;25(6):1128-1134.

108. Ratner BD, Hoffman AS, Schoen FJ, Lemons JE, editors. Biomaterials Science: An Introduction to Materials in Medicine: Academic Press, 2004.

109. Tang L, Ugarova TP, Plow EF, Eaton JW. Molecular determinants of acute inflammatory responses to biomaterials. J Clin Invest 1996 Mar 1;97(5):1329-1334.
110. Muller WA. Leukocyte-endothelial-cell interactions in leukocyte transmigration and the inflammatory response. Trends Immunol 2003 Jun;24(6):327-334.

111. Solovjov DA, Pluskota E, Plow EF. Distinct roles for the alpha and beta subunits in the functions of integrin alphaMbeta2. J Biol Chem 2005 Jan 14;280(2):1336-1345.

112. Nguyen KT, Su SH, Sheng A, Wawro D, Schwade ND, Brouse CF, et al. In vitro hemocompatibility studies of drug-loaded poly-(L-lactic acid) fibers. Biomaterials 2003 Dec;24(28):5191-5201.

113. Suska F, Esposito M, Gretzer C, Kalltorp M, Tengvall P, Thomsen P. IL-1alpha, IL-1beta and TNF-alpha secretion during in vivo/ex vivo cellular interactions with titanium and copper. Biomaterials 2003 Feb;24(3):461-468.

114. DeFife KM, Yun JK, Azeez A, Stack S, Ishihara K, Nakabayashi N, et al. Adhesion and cytokine production by monocytes on poly(2-methacryloyloxyethyl phosphorylcholine-co-alkyl methacrylate)-coated polymers. J Biomed Mater Res 1995 Apr;29(4):431-439.

# BIOGRAPHICAL INFORMATION

Jagannath Dey was born in Calcutta, India in March 1984. He graduated with a Bachelor of Technology degree in Electronics and Communication Engineering from the National Institute of Technology, Trichy, India in May 2005. He worked as a Software Engineer at Flextronics Software Systems, Bangalore, India from Jun 2005 to Aug 2006. After enrolling in the Biomedical Engineering program at the University of Texas at Arlington, he has been actively involved in developing and characterizing different biomaterials with a focus on vascular tissue engineering. His research interests include drug delivery, biomaterials and tissue engineering.